



VCU

Virginia Commonwealth University
VCU Scholars Compass

Theses and Dissertations


Graduate School

2017

CONTRIBUTION OF A CLASS II RIBONUCLEOTIDE REDUCTASE TO THE MANGANESE DEPENDENCE OF *Streptococcus sanguinis*

John L. Smith
Virginia Commonwealth University

Follow this and additional works at: <https://scholarscompass.vcu.edu/etd>

 Part of the [Bacteriology Commons](#), [Cardiovascular Diseases Commons](#), and the [Pathogenic Microbiology Commons](#)

© John Lee Smith

Downloaded from

<https://scholarscompass.vcu.edu/etd/4936>

This Thesis is brought to you for free and open access by the Graduate School at VCU Scholars Compass. It has been accepted for inclusion in Theses and Dissertations by an authorized administrator of VCU Scholars Compass. For more information, please contact libcompass@vcu.edu.

©John Lee Smith, 2017
All rights reserved

Contribution of a Class II Ribonucleotide Reductase to the Manganese dependence of
Streptococcus sanguinis

A thesis submitted in partial fulfillment of the requirements for the degree of Master of
Science at Virginia Commonwealth University

By

John Lee Smith

Religious Studies B.A., University of Mary Washington, 2012

Biology B.S., Virginia Commonwealth University, 2015

Principal Investigator: Dr. Todd Kitten

Associate Professor of Oral and Craniofacial Molecular Biology
and of Microbiology and Immunology

Virginia Commonwealth University

Richmond, VA

June 2017

Acknowledgements

I would like to thank my parents first and foremost for all the love and support. They have pushed the boundaries of what I thought I could achieve. They have always tried to do their hardest to give me the best life I could have, filled with opportunities.

I would like to thank my girlfriend Mary who supported me through my undergrad and graduate programs here at VCU. She has constantly been there to encourage me to pursue my dreams no matter what.

I would like to thank my group of friends, Charlton, Naren, Jerilyn and Zach, who have been through the hardships of school but also there to celebrate the victories.

I would like to thank Dr. Todd Kitten, who took me into his lab as an undergrad student and allowed me to continue my education as a master's student. He has shown me the wonders of oral bacteria and its effect on our bodies.

I would like to thank Dr. Seon-sook, for her help with all my projects and her continuous effort to answer of all my questions.

I would finally like to thank my four kittens who always love me, especially when I am feeding them.

Table of Contents

List of Figures.....	vi
List of Tables.....	viii
List of Abbreviations.....	ix
Abstract.....	xiii
I. Introduction.....	1
A. Streptococci.....	1
B. Viridans streptococci.....	3
C. <i>Streptococcus sanguinis</i>	3
D. Infective Endocarditis.....	4
E. Identification of Virulence Determinants of <i>S. sanguinis</i>	5
F. Lipoproteins.....	6
G. <i>ssaB</i> and <i>ssaACB</i>	7
H. SodA vs <i>ssaB</i>	7
I. Ribonucleotide Reductase (RNR)	8
1. RNR Classes.....	8
2. Anaerobic Class III Ribonucleotide Reductase in <i>Streptococcus sanguinis</i>	11
3. Aerobic Class Ib Ribonucleotide Reductase in <i>Streptococcus sanguinis</i>	11
4. Class II Ribonucleotide Reductase in <i>Lactobacillus leichmannii</i> ..	12

5. Ribonucleotide Reductase Mutants of <i>S. sanguinis</i>	12
6. <i>S. sanguinis</i> Native Cobalamin Biosynthesis Pathway.....	17
7. Spontaneous mutant (SM) of JFP140 ($\Delta nrdHEKF$, $nrdJ^+$).....	17
J. The Purpose of the Study.....	19
Research Objective.....	20
II. Materials and Methods.....	21
A. Broth Preparation: Brain Heart Infusion.....	21
B. Broth Preparation: Chelexed Brain Heart Infusion.....	21
C. Agar Preparation: Brain Heart Infusion plates.....	21
D. Agar Preparation: Antibiotic Brain Heart Infusion plates.....	22
E. Low Melting Point Agar Preparation: Brain Heart Infusion tubes.....	22
F. PCR Purification: MinElute® PCR Purification Kit.....	23
G. MinElute® Gel Extraction Kit.....	23
H. DNA Extraction: QIAGEN© Streptococcal Genomic DNA Preps.....	23
I. DNA Extraction: Modified Chromosomal Mini-prep.....	23
J. Gene SOEing.....	23
K. <i>Streptococcus sanguinis</i> SK36 Transformation Protocol-anaerobic.....	24
L. dNTP extraction for SK36 (WT) JFP227 ($\Delta ssaACB$, ΔSSA_{1413}) and JFP138 ($\Delta nrdHEKF$)	25
III. Results.....	27
A. Replication of the JFP140c (SM $\Delta nrdHEKF$, $nrdJ^+$) plus Cbi growth study	27
B. The Addition of Dimethylbenzimidazole (DMB)	30

C. Addition of Ethanolamine.....	32
D. Gene SOEing to create $\Delta nrdHEKF$, $\Delta nrdI$, $nrdJ^+$	34
E. Ethanolamine effect on 1403 and C3.....	37
F. Addition of 1,2-propanediol.....	38
G. Creation of Spontaneous Mutants.....	40
H. Whole Genome Sequencing.....	45
I. Transformation of JFP140 ($\Delta nrdHEKF$, $nrdJ^+$) with JFP140c (SM $\Delta nrdHEKF$, $nrdJ^+$) <i>fba</i> and JFP140c (SM $\Delta nrdHEKF$, $nrdJ^+$) with JFP140 ($\Delta nrdHEKF$, $nrdJ^+$) <i>fba</i>	52
J. Protein Structure of the <i>fba</i> region in JFP140 ($\Delta nrdHEKF$, $nrdJ^+$) and JFP140c (SM $\Delta nrdHEKF$, $nrdJ^+$).....	55
K. Phenotypic comparison of SK36 (WT), JFP227 ($\Delta ssaACB$, ΔSSA_{1413}) and JFP138 ($\Delta nrdHEKF$)	58
L. Deoxynucleotide analysis of SK36 (WT), JFP138 ($\Delta nrdHEKF$) and JFP227 ($\Delta ssaACB$, ΔSSA_{1413})	61
IV. Discussion.....	62
Literature Cited.....	67
VITA.....	73

List of Figures

Figure 1. Overview of the Ribonucleotide Reductase (RNR) classes.....	10
Figure 2. O ₂ gradient tube assay with WT and RNR mutants.....	15
Figure 3. Replication of JFP140c (SM $\Delta nrdHEKF$, $nrdJ^+$) with Cbi growth assay.....	28
Figure 4. Addition of Ethanolamine to strains SK36 (WT), JFP140 ($\Delta nrdHEKF$, $nrdJ^+$), JFP140c (SM $\Delta nrdHEKF$, $nrdJ^+$), JFP157 ($\Delta nrdI$, $nrdJ^+$) and C3 (SM $\Delta nrdHEKF$, $\Delta nrdI$, $nrdJ^+$), and 1403 ($\Delta nrdHEKF$, $\Delta nrdI$, $nrdJ^+$).....	33
Figure 5. Addition of 1,2-propanediol to strains SK36 (WT), JFP140c (SM $\Delta nrdHEKF$, $nrdJ^+$), JFP157 ($\Delta nrdI$, $nrdJ^+$) and C3 (SM $\Delta nrdHEKF$, $\Delta nrdI$, $nrdJ^+$).....	35
Figure 6. Gene SOEing diagram and primers for the creation of strains 1403 ($\Delta nrdHEKF$, $\Delta nrdI$, $nrdJ^+$) and C3 (SM $\Delta nrdHEKF$, $\Delta nrdI$, $nrdJ^+$).....	36
Figure 7. O ₂ gradient tube assay using 1403 ($\Delta nrdHEKF$, $\Delta nrdI$, $nrdJ^+$) and C3 (SM $\Delta nrdHEKF$, $\Delta nrdI$, $nrdJ^+$).....	39
Figure 8. DAPI staining of JFP140c (SM $\Delta nrdHEKF$, $nrdJ^+$) and SK36 (WT).....	41
Figure 9. O ₂ gradient tube assay using JFP157 ($\Delta nrdI$, $nrdJ^+$) and a potential SM of JFP157 (SM $\Delta nrdI$, $nrdJ^+$).....	43
Figure 10. O ₂ gradient tube assay using JFP163 ($\Delta nrdD$, $nrdJ^+$) and SM JFP163 1.1 (SM $\Delta nrdD$, $nrdJ^+$).....	44

Figure 11. Geneious software image of the SNP in the <i>nox</i> gene for JFP169 1.1 (SM $\Delta nrdD$, $nrdJ^+$).....	49
Figure 12. Geneious software image of the SNP in SSA_1239 for JFP169 1.1 (SM $\Delta nrdD$, $nrdJ^+$).....	50
Figure 13. Geneious software image of the SNP in Fba for JFP140c (SM $\Delta nrdHEKF$, $\Delta nrdI$, $nrdJ^+$).....	51
Figure 14. Transformation of JFP140 ($\Delta nrdHEKF$, $nrdJ^+$) with JFP140c <i>fba</i> and JFP140c (SM $\Delta nrdHEKF$, $nrdJ^+$) with JFP140 <i>fba</i>	54
Figure 15. SWISS-MODEL used to make an alignment with JFP140 ($\Delta nrdHEKF$, $nrdJ^+$) and Methicillin-Resistant <i>Staphylococcus aureus</i> (4to8.1.A)	56
Figure 16. SWISS-MODEL used to make an alignment with JFP140c (SM $\Delta nrdHEKF$, $nrdJ^+$) and Methicillin-Resistant <i>Staphylococcus aureus</i> (4to8.1.A)	57
Figure 17. Phenotypic changes caused by oxygen stress over time on SK36 (WT), JFP227 ($\Delta ssaACB$, ΔSSA_1413) and JFP138 ($\Delta nrdHEKF$)	59

List of Tables

Table 1. Strains used in this study.....	13
Table 2. OD ₆₆₀ Readings of JFP140c (SM $\Delta nrdHEKF$, $nrdJ^+$) with the addition of Cbi.....	29
Table 3. OD ₆₆₀ Readings of JFP140c (SM $\Delta nrdHEKF$, $nrdJ^+$) with the addition of Cbi and DMB.....	31
Table 4. Strains that were whole genome sequenced with Illumina sequencing	47

List of Abbreviations

α	alpha
β	beta
Δ	delta
%	percent
$^{\circ}\text{C}$	degree Celsius
μl	microliter
μg	microgram
A	adenine
ABC	ATP-binding cassette
AdoCbl	adenosylcobalamin (coenzyme B ₁₂)
AdoCob	S-adenosylcobalamine
Asn	asparagine
ATPB	ATP-binding protein
BHI	brain heart infusion
bp	base pair
C	cytosine
Cbi	dicyanocobinamide
CFUs	colony forming units
CI	competitive index
Co	cobalt
CSP	competence stimulating peptide

Cu	copper
Cys	cysteine
DAPI	4',6-diamidino-2-phenylindole
dNDP	deoxyribonucleotide diphosphate
dNTP	deoxyribonucleotide triphosphate
Erm	erythromycin
EtOH	ethanol
Fba	fructose bisphosphate aldolase
Fe	Iron
G	guanine
Gln	glutamine
Gly	glycine
HGT	horizontal gene transfer
His	histidine
HS	horse serum
IMP	integral membrane pretein
IPTG	isopropyl β -D-1-thiogalactopyranoside
Kan	kanamycin
kb	kilobase
LMP	low melting point
MeOH	methanol
ml	milliliter
mM	millimolar

Mn	manganese
NaCl	Sodium Chloride
NDP	ribonucleotide diphosphate
Ni	nickle
nM	nanomolar
NTP	ribonucleotide triphosphate
NVE	native-valve infective endocarditis
OD	optical density
PCR	polymerase chain reaction
RNR	ribonucleotide reductase
ROS	reactive oxygen species
rRNA	ribosomal ribonucleotide acid
SAM	S-adenosylmethionine
SM	spontaneous mutant
SNP	single nucleotide polymorphism
SOEing	gene Splicing by Overlap Extension
Spc	spectinomycin
STM	Signature-tagged mutagenesis
T	thymine
TFA	tissue-factor activity
TH	Todd Hewitt
Thr	threonine
Trp	tryptophan

WT	wild-type
Y [•]	tyrosyl radical
Zn	zinc

ABSTRACT

CONTRIBUTION OF A CLASS II RIBONUCLEOTIDE REDUCTASE TO THE MANGANESE DEPENDENCE OF *Streptococcus sanguinis*

By John Lee Smith

A thesis submitted in partial fulfillment of the requirements for the degree of Master of
Science at Virginia Commonwealth University

Virginia Commonwealth University

Richmond, VA

June 2017

Principal Investigator: Dr. Todd Kitten

Associate Professor of Oral and Craniofacial Molecular Biology

and of Microbiology and Immunology

Manganese-deficient *Streptococcus sanguinis* mutants exhibit a dramatic decrease in virulence for infective endocarditis and in aerobic growth in manganese-limited media. Loss of activity of a manganese-dependent, oxygen-dependent

ribonucleotide reductase (RNR) could explain the decrease in virulence. When the genes encoding this RNR are deleted, there is no growth of the mutant in aerobic broth culture or in an animal model. Testing the contribution of the aerobic RNR to the phenotype of a manganese transporter mutant, a heterologous class II RNR from *Lactobacillus leichmannii* called NrdJ that requires B₁₂ rather than manganese as a cofactor was previously introduced into an RNR mutant of *S. sanguinis*. Aerobic growth was only partially restored. Currently, we sought to improve NrdJ-dependent growth by (i) amending the medium to increase cellular levels of B₁₂; (ii) characterizing a spontaneous mutant of the NrdJ-complemented strain with improved aerobic growth; and (iii) altering this strain through further genetic manipulation.

I. INTRODUCTION

A. Streptococci

In 1874 an Austrian surgeon, Theodor Billroth, first described a streptococcal infection in erysipelas, a bacterial infection of the outer layer of the skin which is usually associated with a skin rash and wound infections (1,2). He described the bacteria observed as streptococci meaning a chain (strepto) and berry (coccus). In 1879 streptococci became officially known due to Louis Pasteur and his isolation of the causative agent of the disease puerperal fever (3). Puerperal fever is a postpartum infection that was often fatal during this time period (4).

In 1903, Hugo Schottmuller created the blood agar plate that helped to differentiate streptococci (5,6). His work was in differentiating between hemolytic and nonhemolytic strains of the bacteria (21). James Howard Brown described the three types of hemolytic patterns in 1919. An alpha hemolytic pattern is a green zone of discoloration, whereas a beta hemolytic pattern is a clear zone and a gamma hemolytic pattern indicates no change. Alpha patterns were characteristic of viridans streptococci, beta were characteristic of *S. haemolyticus* type organisms and gamma were characteristic of enterococci (4).

In 1933, Rebecca Lancefield reported a method of differentiating beta-hemolytic streptococcal strains. The method worked by categorizing the *Streptococcus* based on the carbohydrate composition of the antigens in the cell wall (21). Building on this work J. M. Sherman further broke down streptococci into four groups. They were viridans, enterococci, lactic and pyogenic groups (8). These groups, still used today, were based

on hemolytic reaction, Lancefield grouping, and phenotypic tests, primarily fermentation and tolerance (21).

The streptococcal species that were placed in the pyogenic division were beta-hemolytic with the Lancefield groupings A, B, C, E, F, and G. This system has not changed significantly with the modern serotyping (22). The lactic division encompassed all the strains that were associated primarily with the manufacturing of dairy products. These strains were renamed *Lactococcus* in the 1930s. The traditional lactic group was not beta-hemolytic and grew at 10°C. It did not grow at 45°C and also failed to grow at 6.5% NaCl. The strains were not associated with human infections but with the reclassification there have been newly discovered strains that do infect humans (22). Enterococci exhibit varied beta-hemolysis. However, those that are in this division are tolerant to high pH, high salt concentration and grow from temperatures as low as 10°C and as high as 45°C (22). Finally, viridans streptococcus strains are not beta-hemolytic and are not able to grow in high-pH conditions, nor can they grow on high salt concentrations or at 10°C (22).

Historically, the classification of bacterial isolates has been dependent on morphological and phenotypic similarities with type strains. However, this method of categorizing bacteria was less than perfect. In the 1980s, laboratories of Woese and others were starting to use the stable genetic codes found in the 5S, 16S, 23S rRNA and the spaces between these genes to start to classify bacteria genetically (23). The 16S rRNA is now the genetic area that is most often used in taxonomy of bacteria (23).

B. Viridans streptococci

Viridans streptococci are gram positive cocci arranged in chains. They are catalase-negative, leucine aminopeptidase positive, pyrrolidonylarylamidase negative and have no growth in 6.5% NaCl broth. Viridans streptococci received their name from their green color in response to the alpha-hemolysis that occurs on blood agar. However, because not all of the viridans streptococci perform alpha-hemolysis, this group is also known as oral streptococci. This name also does not accurately describe the group since some species come from the gastrointestinal, vaginal and dairy product sources (21). Viridans is further divided into five subcategories. These are the *Streptococcus mutans* group, *Streptococcus salivarius* group, *Streptococcus anginosus* group, *Streptococcus mitis* group and *Streptococcus sanguinis* group (formerly *S. sanguis*) (21).

C. *Streptococcus sanguinis*

Streptococcus sanguinis was previously called *Streptococcus sanguis*. In 1997, *Streptococcus sanguis*, meaning “the blood”, was changed to the more grammatically correct *Streptococcus sanguinis*, meaning “of the blood” (9). *Streptococcus sanguinis* is a gram-positive, facultative anaerobe and normally found in the human mouth (16). As a primary colonizer of the mouth, in infants *S. sanguinis* is the first bacterium to emerge within the oral cavity and it correlates to the emergence of the first tooth, at around nine months of age (10). In adults, during the first four hours after a professional cleaning, the majority of the cultivable bacteria are streptococci (11). *S. sanguinis* adheres to components within the salivary pellicle, which is a thin coating that covers

the tooth surface. Many of the components consist of glycoproteins, mucins and enzymes found in saliva (12).

If nothing else, *S. sanguinis* could be described as a benign indicator of a healthy oral cavity. At its best, *S. sanguinis* could be a beneficial bacterium in the mouth (10). *S. sanguinis* has an antagonistic interaction with *Streptococcus mutans*, a well-known cause of caries within the oral cavity (13). *S. sanguinis* produces hydrogen peroxide that impedes the growth of *S. mutans*, so a high ratio of *S. mutans* to *S. sanguinis* is a common indicator of poor health in the mouth (13).

An unfortunate truth is that oral streptococci and staphylococci account for most cases of infective endocarditis if they enter the bloodstream (14). *S. sanguinis* is commonly the culprit for causing infective endocarditis from the viridans species (15).

D. Infective Endocarditis

Infective endocarditis, when caused by *S. sanguinis*, is commonly categorized as a native-valve infective endocarditis (NVE) (14, 16). Native-valve infective endocarditis is traditionally associated with congenital heart disease, chronic rheumatic heart disease and mitral valve prolapse with regurgitation (14, 16). Platelets and fibrin accumulate on the damaged valve. The result is the formation of a sterile “vegetation.” Bacteria can then accumulate on top of the platelets and fibrin layer which in turn attracts monocytes, activating tissue-factor activity (TFA) and cytokines (16). More platelets and fibrin attach to the bacteria; some of the bacteria seed the bloodstream and attach to the surface of the newly formed vegetation and the process continues, supporting additional vegetative growth (16). Infective endocarditis is still a challenging

disease to manage and continues to have a high mortality rate even with advances in technology (17). Viridans streptococci are the predominant cause of NVE (55.1%) (19). In one study, the most common species of oral streptococci leading to infective endocarditis were *Streptococcus sanguis* sensu stricto (31.9%), *S. oralis* (29.8%) and *S. gordonii* (12.7%) (18). However, these percentages and species can fluctuate from study to study. Oral streptococci can enter the bloodstream from dental procedures but also from eating or basic oral care. This would indicate that antibiotics are not the best solution and would prompt the need for a vaccine or some other protective measure (16).

E. Identification of Virulence Determinants of *S. sanguinis*

Since *S. sanguinis* causes endocarditis there was a need to discover the genes that cause virulence that could be used for a potential vaccine or drug target. Signature-tagged mutagenesis (STM) technique was used to search for virulence factors for endocarditis. Using 800 mutants of *S. sanguinis* SK36, STM identified 38 putative avirulent and 5 putative hypervirulent mutants (16). There were six mutants that appeared to be the most promising. The mutations were in genes encoding undecaprenol kinase, homoserine kinase, anaerobic ribonucleotide reductase (RNR), adenylosuccinate lyase, a hypothetical protein and an intergenic region (16).

A surface bound protein would be necessary for a vaccine. Bioinformatics were used to find 52 putative lipoproteins (20). STM was used to systematically knock out these lipoproteins one by one. Knockout mutants were then compared to wild-type SK36 using a competitive index (CI) assay to show whether the mutant was more, less

or similarly virulent (20). A rabbit model was used for the CI assay. Cardiac catheterization caused the formation of sterile vegetations and then a 1:1 inoculation of the wild-type and mutant was injected into the animal model. The vegetation was then plated and compared to the initial inoculum to create the competitive index ratio.

F. Lipoproteins

Within streptococcal species, lipoproteins have been known to contribute to virulence, which makes the targeting of lipoproteins a viable vaccine option (20). These lipoprotein virulence functions include adhesion, posttranslational modification and ATP-binding cassette (ABC) mediated transport (20). Of the 52 putative lipoprotein mutants, only six were found to have reduced virulence during the STM screen. The six mutated genes were SSA_0004, SSA_0588, SSA_1122, SSA_1976, SSA_2243, and *ssaB*. Along with the six mutants two lipoprotein related genes were tested, *lgt* and *lspA*, both mutants of which also were found to have reduced virulence. Of the eight mutants only three were significantly less competitive using the competitive index assay, those with mutations in prolipoprotein diacylglyceryl transferase (*lgt*) which is a lipoprotein-processing enzyme, signal peptidase II (*lspA*) also a lipoprotein-processing enzyme and a manganese ABC transporter substrate-binding protein (*ssaB*) (20). Only the *ssaB* mutant displayed a signal that had the same signal intensity as the negative control and had reduced competitiveness in the CI assay. Additionally, the drop in virulence for the *lgt* and *lspA* mutants was only twofold to threefold in the animal model while the *ssaB* mutant had a drop of over 1,000-fold (20).

G. *ssaB* and *ssaACB*

The lipoprotein SsaB (SSA_0260) belongs to the lipoprotein receptor antigen I (Lral) family of conserved metal transporters. Lral operons minimally contain the genes for an ATP-binding protein (ATPB), an integral membrane protein (IMP) and the Lral lipoprotein (24). The Lral operon within *Streptococcus pneumoniae*, *Streptococcus gordonii*, *Streptococcus parasanguinis*, other streptococci and even in a cyanobacterium are believed to transport Mn and maybe to a lesser extent iron (25, 24). In addition, *ssaR* (SSA_0256) which is a MntR, a manganese-dependent transcriptional regulator, is encoded in close proximity to the Lral operon, *ssaACB*, in order to repress the uptake of manganese when it is in abundance (25). The deletion of *ssaB* or the more complete deletion of the whole operon, *ssaACB*, caused a decrease in virulence and aerobic growth in manganese-limited media, presumably due to the decrease of manganese that is able to enter the cell (25). Restoration of aerobic growth for the *ssaB* mutant was seen with the addition of manganese but not with other divalent metal ions: iron, cobalt, copper, nickel or zinc (Fe^{2+} , Co^{2+} , Cu^{2+} , Ni^{2+} or Zn^{2+}) (25).

H. SodA vs *ssaB*

The deletion of *ssaB* was seen in vitro to decrease growth in aerobic conditions but not when oxygen levels are low. The potential reason for this decline could be due to the decrease in activity of SodA, the manganese-dependent superoxide dismutase (25). However, deletion of *sodA* revealed that the *sodA* mutant is only 10-fold less competitive than the wild-type in the rabbit model of endocarditis while the *ssaB* mutant is over 1000-fold less competitive using a CI assay (25). In an in vitro model using rabbit

serum at 12% O₂, the *sodA* mutant was decreased by a factor of a 1000 in growth while the *ssaB* mutant was decreased by a factor of a 100,000 in growth. This would indicate that the decrease in virulence with the deletion of *ssaB*, which causes a decrease in manganese uptake, is not due solely to loss of SodA activity.

I. Ribonucleotide Reductase (RNR)

1. RNR Classes

One of the major enzymes that uses manganese within *Streptococcus sanguinis* is ribonucleotide reductase. Ribonucleotide reductase (RNR) is the only enzyme that can synthesize deoxyribonucleotide triphosphate (dNTP) through a *de novo* biochemical pathway. This enzyme is needed for the conversion of ribonucleotides to deoxyribonucleotides which is needed for DNA replication and repair (26). There are three classes of RNR for the conversion of ribonucleotide diphosphates (NDP) or ribonucleotide triphosphates (NTP) to deoxyribonucleotide diphosphates (dNDP) or deoxyribonucleotide triphosphates (dNTP) respectively: class I, class II and class III. Class I is divided into three subgroup classes which are dependent on the metal cofactor they use (26). Class Ia uses a di-iron center (Fe^{III}-O-Fe^{III}), class Ib uses a di-manganese center (Mn^{III}-O-Mn^{III}) *in vivo* but was able to work with a di-iron center (Fe^{III}-O-Fe^{III}) *in vitro*, and class Ic uses a manganese iron center (Mn^{IV}-O-Fe^{III}) (26). All three subgroups convert NDPs to dNDPs and require the presence of oxygen for the generation of a radical catalyst (26).

Class II uses S-adenosylcobalamine (AdoCob), also known as vitamin B₁₂, as a cofactor to convert both NDP and NTP to dNDP and dNTP respectively. Class II is also oxygen independent and can be used for both aerobic and anaerobic growth (26).

Class III requires the binding of S-adenosylmethionine (SAM) to an iron-sulfur cluster ([4Fe-4S]⁺) to catalyze the reaction from NTP to dNTP. This class is only active under anaerobic conditions (26). A summary of these RNR classes is illustrated in Figure 1.

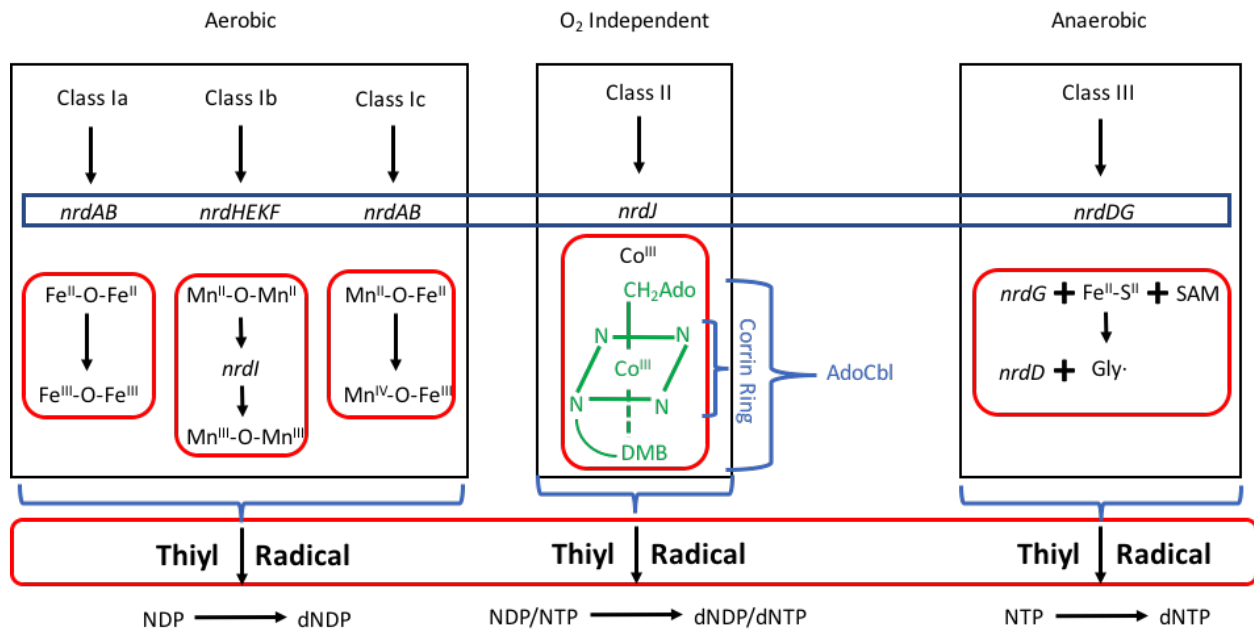


Figure 1. Overview of the Ribonucleotide Reductase (RNR) classes. Class I RNR are all aerobic and split into three subclasses. Class Ia uses NrdAB and iron (Fe) is the metallo-cofactor. Class Ib uses NrdHEKF and manganese (Mn) is the metallo-cofactor in vivo. The transition of the Mn to a tyrosyl radical needs NrdI. The class Ic uses NrdAB and the metallo-cofactor is Fe and Mn. Class I RNRs need oxygen to create the tyrosyl radical to then create the thiyl radical which converts NDP to dNDP. Class II is O₂ independent and uses NrdJ. The metallo-cofactor is cobalt (Co) and the enzyme uses the cofactor adenosylcobalamin (AdoCbl) to create the thiyl radical. Class II RNR can convert both NDP and NTP to dNDP and dNTP. Class III is strictly anaerobic using NrdDG. NrdG requires S-adenosylmethionine (SAM) and an iron-sulfur cluster to create a glycy radical. NrdD then uses the glycy radical to create the thiyl radical to convert NTP to dNTP.

2. Anaerobic Class III Ribonucleotide Reductase in *Streptococcus sanguinis*

Streptococcus sanguinis possesses an anaerobic class III RNR (27). The proteins that comprise the anaerobic class III RNR are NrdD, alpha (α) subunit, and NrdG, the beta (β) subunit, which must form a homodimer to become active (26). NrdD has the active site while NrdG is the activase (26) using S-adenosylmethionine (SAM) and the iron-sulfur cluster ($[4\text{Fe-4S}]^+$) to form a glycy radical (28). NrdDG can only be formed under strictly anaerobic conditions because the $[4\text{Fe-4S}]^+$, glycy radical, and SAM rapidly degrade in the presence of oxygen (27). NrdD is permanently inactivated through the cleavage of the polypeptide chain (27). The class III RNR does not use manganese and cannot be activated in the presence of oxygen. These two factors should exclude NrdDG as a possibility for the decrease in virulence when *ssaB* or *ssaACB* are deleted and the mutant is grown aerobically.

3. Aerobic Class Ib Ribonucleotide Reductase in *Streptococcus sanguinis*

Streptococcus sanguinis possesses an aerobic class Ib RNR which uses Mn *in vivo*. The decrease in aerobic virulence upon deletion of the *ssaB/ssaACB* genes encoding a Mn transporter, could be related to the aerobic Mn-dependent RNR, which is encoded by *nrdHEKF* (26). The α subunit is NrdE while NrdF is the β subunit. Both α and β each form two homodimeric subunits. The α subunit is the catalytic subunit where the nucleotide reduction occurs, and the β subunit contains the di-manganese center (Mn^{II}_2) that oxidizes a conserved cysteine in the active site of the enzyme to form the thiyl radical (26, 29). NrdI is a flavodoxin that oxidizes the Mn^{II}_2 -NrdF to the active Mn^{III}_2 -

Y[•] (27, 29). NrdH is a glutaredoxin-like thioredoxin that reduces the disulfide formed by the conversion of the NDP to dNDP or NTP to dNTP (27). NrdK is a hypothetical protein of unknown function (27).

4. Class II Ribonucleotide Reductase in *Lactobacillus leichmannii*

NrdJ is the essential protein for the class II RNR and is comprised of a single α -chain polypeptide (26). NrdJ is the α subunit with the active center containing the allosteric sites of the enzyme, and S-adenosylcobalamin (AdoCob) is used as the “ β subunit” to generate the thiyl radical (26, 27). NrdJ is oxygen-independent and can use both NDPs and NTPs as substrates (26).

5. Ribonucleotide Reductase Mutants of *S. sanguinis*

The first RNR mutant was created by replacing *nrdHEKF*, encoding the class Ib RNR, with the *aphA-3* gene encoding kanamycin resistance (Kan^r) and named JFP138 ($\Delta nrdHEKF$) (27). Strains used for this study are listed in Table 1. Additionally, a mutant was created by replacing *nrdI* with the *aphA-3* gene encoding Kan^r and named JFP143 ($\Delta nrdI$). Both JFP138 ($\Delta nrdHEKF$) and JFP143 ($\Delta nrdI$) failed to grow aerobically; however, they both grew anaerobically (27).

JFP138 ($\Delta nrdHEKF$) was then complemented with *nrdJ*, encoding the oxygen independent class II RNR from *L. leichmannii*, behind an Isopropyl β -D-1-thiogalactopyranoside (IPTG) inducible promoter (27). This mutant was designated JFP140 ($\Delta nrdHEKF, nrdJ^+$) (27). JFP143 ($\Delta nrdI$) was also complemented with *nrdJ* and named JFP157 ($\Delta nrdI, nrdJ^+$) (27).

Table 1 Strains used in this study

Strains	Description
<i>S. sanguinis</i> SK36	WT isolate from human dental plaque; virulent in rat and rabbit models of infective endocarditis
JFP140	Kan ^r Spc ^r ; $\Delta nrdHEKF::aphA-3$ SSA_0169:: <i>aad9</i> Phyper-spank <i>lacZo nrdJ lacI</i>
JFP140c	Spontaneous mutant of JFP140; Kan ^r Spc ^r ; $\Delta nrdHEKF::aphA-3$ SSA_0169:: <i>aad9</i> Phyper-spank <i>lacZo nrdJ lacI</i>
1403	JFP140 deleted for <i>nrdI</i> ; Kan ^r Erm ^r Spc ^r ; $\Delta nrdHEKF::aphA-3$ $\Delta nrdI::ermB$ SSA_0169:: <i>aad9</i> Phyper-spank <i>lacZo nrdJ lacI</i>
C3	JFP140c deleted for <i>nrdI</i> ; Kan ^r Erm ^r Spc ^r ; $\Delta nrdHEKF::aphA-3$ $\Delta nrdI::ermB$ SSA_0169:: <i>aad9</i> Phyper-spank <i>lacZo nrdJ lacI</i>
JFP138	Kan ^r ; $\Delta nrdHEKF::aphA-3$
JFP227	JFP173 deleted for SSA_1413; Tet ^r Kan ^r ; $\Delta ssaACB::tetM$ $\Delta SSA_1413::aphA-3$
JFP169	Kan ^r ; $\Delta ssaACB::aphA-3$
JFP173	Tet ^r ; $\Delta ssaACB::tetM$
JFP157	Kan ^r Spc ^r ; $\Delta nrdI::aphA-3$ SSA_0169:: <i>aad9</i> Phyper-spank <i>lacZo nrdJ lacI</i>
JFP163	Cm ^r Spc ^r ; <i>nrdD::magellan2</i> SSA_0169:: <i>aad9</i> Phyper-spank <i>lacZo nrdJ lacI</i>
JFP36	Erm ^r ; SSA_0169:: <i>ermB</i>
JFP143	Kan ^r ; $\Delta nrdI::aphA-3$

Despite the addition of *nrdJ*, the strains JFP140 ($\Delta nrdHEKF$, *nrdJ*⁺) and JFP157 ($\Delta nrdI$, *nrdJ*⁺) failed to grow to wild-type, SK36, levels when induced with IPTG. The strains did, however, grow better than their non-complemented counterparts, JFP138 ($\Delta nrdHEKF$) and JFP143 ($\Delta nrdI$) respectively (27) (Fig 2).

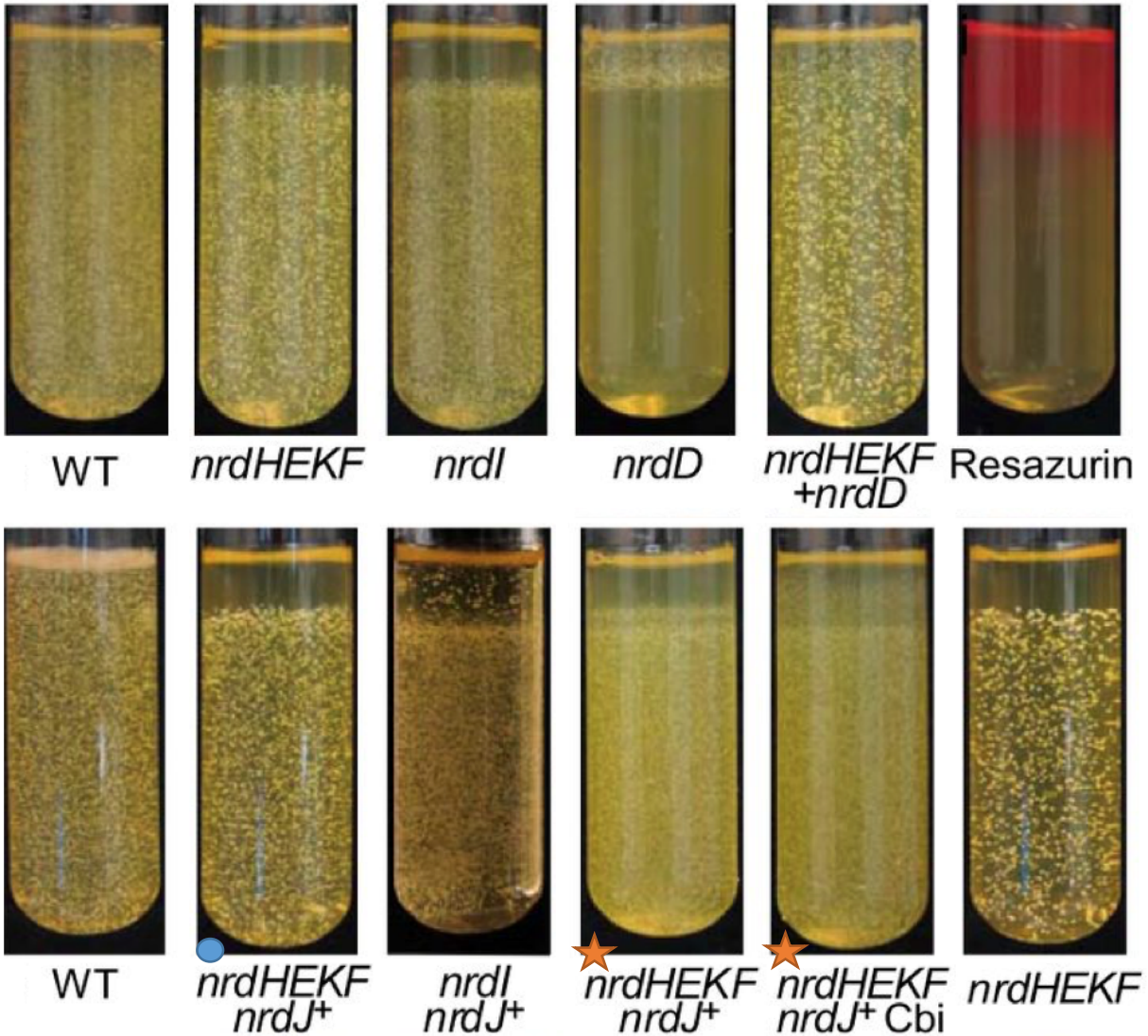


Figure 2. O₂ gradient tube assay with WT and RNR mutants. Tubes were filled with BHI containing low melting point agarose (LMP) and allowed to become anaerobic, in an anaerobic chamber. After the tubes become anaerobic they were inoculated and allowed to solidify in the anaerobic chamber before being transferred to an aerobic incubator at 37°C. The Resazurin tube contained 5 µg/ml resazurin; the red in the tube indicated the aerobic region while the clear area is the anaerobic region. The class III deletion mutant, labeled *nrdD*, fails to grow anaerobically. All strains with *nrdJ* were

grown with 100 μ m IPTG and the *nrdHEKF nrdJ⁺* Cbi tube had 320 nm of Cbi, final concentration, added to the tube. The tubes marked with an orange star are both JFP140c (SM Δ *nrdHEKF, nrdJ⁺*) The tube marked with a blue circle contains JFP140 (Δ *nrdHEKF, nrdJ⁺*). Image adapted from Rhodes, D. V., Crump, K. E., Makhlynets, O., Snyder, M., Ge, X., Xu, P., Stubbe, J., Kitten, T.

6. *S. sanguinis* Native Cobalamin Biosynthesis Pathway

Streptococcus sanguinis has a 70-kb cluster of 68 genes likely acquired by horizontal gene transfer (HGT; SSA_0463 to SSA_0541) which encodes an anaerobic cobalamin biosynthesis pathway (*cob*), a propanediol utilization pathway (*pdu*) and an ethanolamine utilization pathway (*eut*) (30). Enzymes that catabolize 1,2-propanediol and ethanolamine require coenzyme B₁₂ and these pathways play an important role in *Salmonella* species (30). Also *S. sanguinis*, SK36, has a putative *rli55* orthologous with B₁₂ riboswitches, ANTAR elements and terminator that could regulate ethanolamine utilization and B₁₂ biosynthesis (31). The fact that SK36 has kept this large 70-kb HGT region and that *nrdJ* partially complements a *nrdHEKF* deletion indicates that cobalamin (B₁₂) is being synthesized.

7. Spontaneous mutant of JFP140 ($\Delta nrdHEKF$, *nrdJ*⁺)

Because *nrdJ* was not completely complementing the deleted native class Ib RNR, adenosylcobalamin (coenzyme B₁₂) (AdoCbl) or dicyanocobinamide (Cbi) was added to cultures to see if the addition would increase growth by potentially providing AdoCbl for NrdJ or a component of coenzyme B₁₂, Cbi, to stimulate NrdJ function (27). The addition of AdoCbl to the cultures had no effect at concentrations of 10, 15, 50 and 150 nM. This may be due to the possibility that SK36 does not have an AdoCbl transporter. The incorporation of Cbi at concentrations of 5 to 80 nM had no effect and concentrations of 160, 320 and 640 nM inhibited growth (27). However, one culture of JFP140 ($\Delta nrdHEKF$, *nrdJ*⁺) at 320 nM after 48 hours of incubation had an OD₆₆₀ comparable to wild-type (27). This spontaneous mutant was named JFP140c (SM

ΔnrdHEKF, nrdJ⁺) and seemed to have an increase in growth when 320 nM of Cbi was added to the growth media (27). A tube assay of select RNR mutants is shown in Figure

2.

J. The Purpose of the Study

The class II gene *nrdJ* failed to completely complement the native aerobic Mn dependent RNR due to reasons that are not completely understood. One purpose of this study was to discover a way to enhance the growth of the *nrdJ*-complemented strains and potentially discover the reason why *nrdJ* is not allowing the mutants to grow to wild-type levels. Once a mutant without the native aerobic RNR grows to WT levels, the *ssaACB* gene can be deleted in this mutant. This new mutant could be tested and if there is no decrease in virulence then we would know that the aerobic Ib RNR is the reason for the decrease in virulence when the gene for the Mn transporter, *ssaB*, is deleted. However, if there is still a decrease in virulence, then the aerobic Ib RNR is not the cause for the decrease in virulence with the deletion of *ssaB*. Another independent approach to address this question is to compare phenotypes exhibited by the *nrdHEKF* mutant when placed under aerobic conditions to that of a manganese-deficient mutant. If loss of Mn-dependent RNR activity is responsible for loss of aerobic growth in a Mn-transporter mutant, then any phenotypes displayed by the RNR mutant should be shared by the transporter mutant. In contrast, if the RNR mutant and transporter mutant stop growing for different reasons, then we would expect to see phenotypic differences.

Research Objective

The Aim of this Study is:

To determine whether manganese-deficient *Streptococcus sanguinis* cells fail to grow under aerobic conditions due to reduced activity of the manganese-dependent aerobic class Ib RNR. Two independent approaches will be used to address this question:

1. Attempt to create a strain that can synthesize deoxynucleotides in the absence of the native class Ib RNR. This will be accomplished by characterizing existing strains lacking the class Ib RNR and introducing into them the manganese-independent Class II RNR from *Lactobacillus leichmannii*. These experiments will include spontaneous mutants that grow better aerobically than their parent strains. New strains will also be created. If this is accomplished as expected, the *ssaACB* manganese transporter will be deleted to determine whether manganese depletion reduces virulence to the same extent in a strain that doesn't require manganese for deoxynucleotide synthesis.

2. Compare a manganese-deficient strain of *S. sanguinis* to a strain deleted for the class Ib RNR to see if the two strains possess similar phenotypes. The microscopic morphology of the transporter mutant and the *nrdHEKF* mutant will be compared. In addition, nucleotide pool analysis will be performed to determine whether the transporter mutant is depleted for deoxynucleotides.

II. MATERIALS AND METHODS

A. Broth Preparation: Brain Heart Infusion

Seven and four tenths grams of Bacto™ BHI powder (BD Diagnostic Systems) was dissolved in 200 mL deionized H₂O using a stir bar for mixing on a hot plate. The stir bar was removed with a magnet and the media was autoclaved for 25 minutes at 121°C. The Pyrex® glass bottle of media was then covered in aluminum foil and stored at room temperature. Media was discarded after two weeks to maintain consistent results.

B. Broth Preparation: Chelexed Brain Heart Infusion

Seven and four tenths grams of Bacto™ BHI powder was dissolved in 200 mL deionized H₂O using a stir bar for mixing on a hot plate. Sixteen grams of Chelex per 200 mL was added and allowed to stir for 90 minutes. The stir bar was removed with a magnet and the media was filter sterilized. One mM calcium and magnesium were added back to the media. The plastic bottle of media was then covered in aluminum foil and stored at room temperature. Media was discarded after two weeks to maintain consistent results.

C. Agar Preparation: Brain Heart Infusion plates

Seven and four tenths grams of Bacto™ BHI powder was dissolved in 200 mL deionized H₂O using a stir bar for mixing on a hot plate. The media was autoclaved for 25 minutes at 121°C. The Pyrex® glass bottle was placed in a 56°C water bath to cool.

18 mL was poured out into 11 Petri dishes. Plates were poured and allowed to cool and solidify in a Labconco BSL-2 hood and stored inverted at 4°C.

D. Agar Preparation: Antibiotic Brain Heart Infusion plates

Seven and four tenths grams of BHI powder was dissolved in 200 mL deionized H₂O using a stir bar for mixing on a hot plate. The media was autoclaved for 25 minutes at 121°C. The Pyrex® glass bottle was placed in a 56°C water bath to cool then antibiotics were added to the media and mixed with the stir bar that remained in the glass jar. Eighteen mL was poured out into each of 11 Petri dishes. Plates were poured and allowed to cool and solidify in a Labconco BSL-2 hood and stored inverted at 4°C.

E. Low Melting Point Agar Preparation: Brain Heart Infusion tubes

Eighteen-mL glass tubes with candy cane-shaped aluminum foil tops designed to allow gas exchange were autoclaved for 25 minutes at 121°C. Three and seven tenths grams of BHI powder and 1.0 gram of analytical grade LMP agarose (Promega) was dissolved in 100 mL deionized H₂O using a stir bar for mixing on a hot plate. The media was autoclaved for 25 minutes at 121°C. The Pyrex® glass bottle was placed in a 60°C water bath to cool. The media was mixed a final time and 10 mL of media was placed in each of the ten tubes under a Labconco BSL-2 hood. The tubes were quickly filled and quickly placed in the anaerobic chamber at 37°C. Two days were needed for the tubes to become completely anaerobic before they were inoculated and allowed to solidify at room temperature but remained in the anaerobic chamber until solid. Once solid, the

tubes were taken out of the anaerobic chamber and incubated aerobically at 37°C.
Growth could be seen in 24 to 48 hours.

F. PCR Purification: MinElute® PCR Purification Kit

The QIAGEN© MinElute® PCR Purification Kit, Cat. No. 28004, protocol was followed except that step 7 used 15 µl of deionized H₂O instead of Buffer EB.

G. MinElute® Gel Extraction Kit

The QIAGEN© MinElute® Gel Extraction Kit, Cat. No. 28604, protocol was followed.

H. DNA Extraction: QIAGEN© Streptococcal Genomic DNA Preps

The QIAGEN© DNeasy® Blood and Tissue Kit, Cat. No. 69504, protocol was followed.

I. DNA Extraction: Modified Chromosomal Mini-prep

The modified chromosomal mini-prep protocol was followed, as described in “Genetic Characterization of a *Streptococcus mutans* Lral Family Operon and Role in Virulence” (24).

J. Gene SOEing

Gene SOEing protocol was followed as described in “PCR-mediated recombination and mutagenesis. SOEing together tailor-made genes” (35).

K. *Streptococcus sanguinis* SK36 Transformation Protocol-anaerobic

First a tube of 12.675 ml Bacto™ Todd Hewitt broth (TH) was obtained from the freezer, prepared as described in Paik et al., 2005 (16). A 1-ml aliquot of horse serum (HS) was obtained from the freezer and 325 µl was transferred to the tube of TH, creating 13 ml of TH+HS. Two ml TH+HS were transferred to a BD Falcon™ snap-cap tube and 1 ml to a microfuge tube. A frozen aliquot was used, JFP140 ($\Delta nrdHEKF$, $nrdJ^+$) or JFP140c (SM $\Delta nrdHEKF$, $nrdJ^+$), to inoculate the 2 ml tube. Then all the tubes were incubated overnight at 37°C in the anaerobic chamber. BHI plates were prepared with Kan and Spc antibiotics added to the media.

The next day, 50 µl of the overnight culture were transferred to 10 ml TH+HS and returned to the 37°C incubator. Also, the OD₆₀₀ of the overnight culture was measured against the 1-ml TH+HS blank. It was around 0.8-0.9. Prior to transformation, around 10 ng of JFP140 ($\Delta nrdHEKF$, $nrdJ^+$) FBA DNA or 10 ng of JFP140c (SM $\Delta nrdHEKF$, $nrdJ^+$) FBA DNA and 2 ml (70 ng) of competence stimulating peptide (CSP) were placed in sterile 0.7-ml microfuge tubes and placed in the anaerobic chamber in the 37°C incubator to pre-warm. The diluted culture was incubated at 37°C for 3 hrs. The OD₆₀₀ was measured after the 3-hour incubation and it was <0.1. Three hundred and thirty µl of cell culture was transferred to each microfuge tube with the DNA and CSP and incubated for 4 hours. After the 4-hour incubation the 2 transformations, JFP140 ($\Delta nrdHEKF$, $nrdJ^+$) transformed using JFP140c (SM $\Delta nrdHEKF$, $nrdJ^+$) FBA DNA and JFP140c (SM $\Delta nrdHEKF$, $nrdJ^+$) transformed using JFP140 ($\Delta nrdHEKF$, $nrdJ^+$) FBA DNA, were plated on the BHI plates with kan and spc antibiotics added. Plates were then placed in an anoxomat jar in 0% O₂ and incubated at 37°C for one day.

L. dNTP extraction for SK36 (WT), JFP227 (Δ ssaACB, Δ SSA_1413) and JFP138 (Δ nrdHEKF)

Pre-cultures were made in the anaerobic chamber with 5 ml of anaerobic BHI broth incubated overnight at 37°C. A frozen aliquot was used, SK36, JFP227 (Δ ssaACB, Δ SSA_1413) and JFP138 (Δ nrdHEKF), to inoculate the pre-culture tubes. Three 19 ml tubes filled with uninoculated BHI broth, one for each strain, were pre-incubated anaerobically in the incubator, 37°C. Three baffled flasks with 15 ml of aerobic BHI were pre-incubated at 37°C aerobically.

The next morning, 1 ml of JFP227 (Δ ssaACB, Δ SSA_1413) was added to one tube of 19 ml of BHI (1:20 dilution) and incubated for 3.5 hours anaerobically at 37°C. One and a half hours after JFP227 (Δ ssaACB, Δ SSA_1413) was inoculated, 1 ml of SK36 (WT) was added to one tube of 19 ml of BHI (1:20 dilution) and incubated for 2 hours anaerobically at 37°C. At the same time as SK36 (WT), 1 ml of JFP138 (Δ nrdHEKF) was added to one tube of 19 ml of BHI (1:20 dilution) and incubated for 2 hours anaerobically at 37°C. After the incubation period, 5 ml of each strain was added to 15 ml BHI in a 250-ml baffled flask (1:4 dilution) and incubated at 37°C in an aerobic shaker for 2 hours. Each culture, 20 ml, was placed in a 50 ml tube and all 3 tubes placed in -80°C 100% ethanol (EtOH) until the contents were about to freeze. The tubes were centrifuged in 4°C at max speed for 10 minutes. The supernatant was poured off and the pellet was resuspended in 250 μ l 70% methanol (MeOH) and transferred to a screw top microfuge tube. The tubes were placed in a 5°C water bath for three to five minutes. Tubes were then placed in a 25°C centrifuge and spun for 3 minutes at max speed. The supernatant was collected and a speedvac was used to dry out the

contents. The tubes were stored at -80°C and mailed on dry ice to Dr. Kim Baek at Emory University for analysis of the dNTP levels within the mutants and WT.

III. Results

A. Replication of the JFP140c (SM $\Delta nrdHEKF$, $nrdJ^+$) plus Cbi growth study

The first experiment done was the replication of increasing the growth of JFP140c (SM $\Delta nrdHEKF$, $nrdJ^+$) with the addition of Cbi, as done previously (27).

The pre-culture for JFP140c (SM $\Delta nrdHEKF$, $nrdJ^+$) was grown in 5 ml of BHI broth with the addition of Kan (500 $\mu\text{g/ml}$), Spc (200 $\mu\text{g/ml}$) and 1 mM of IPTG in an anaerobic chamber at 37°C. After incubating for 16-18 hours the pre-culture was diluted 10^{-6} -fold and inoculated into 5 mL aerobic BHI broth with 1 mM of IPTG plus varying concentrations of Cbi; 0 nM, 10 nM, 20 nM, 40 nM, 80 nM, 160 nM and 320 nM. These cultures were incubated at 6% O₂ in an Anoxomat Jar at 37°C for 24 hours. These cultures were then sonicated and plated using a spiral plater on BHI agar. The bacteria were allowed to grow on the plates anaerobically at 37°C and colonies counted after 24 hours of incubation. There was no effect on growth for concentrations of 10 nM, 20 nM, and 40 nM Cbi. There was a slight inhibitory effect at 80 nM, a moderate inhibitory effect at 160 nM and no growth at 320 nM (Fig. 3). In summary, there was no increase in growth at any concentration with the addition of Cbi and only an inhibitory effect at the higher concentrations.

Cbi was added to JFP140c (SM $\Delta nrdHEKF$, $nrdJ^+$) multiple times except cultures were assayed for OD₆₆₀ (Table 2) instead of being plated. Consistently, JFP140c (SM $\Delta nrdHEKF$, $nrdJ^+$) grew at concentrations of 40 nM and below very similarly to 0 nM of Cbi. However, there was a slight (0.010 to 0.030 OD units) increase in OD₆₆₀ around concentrations of 20 to 40 nM Cbi in most cases.

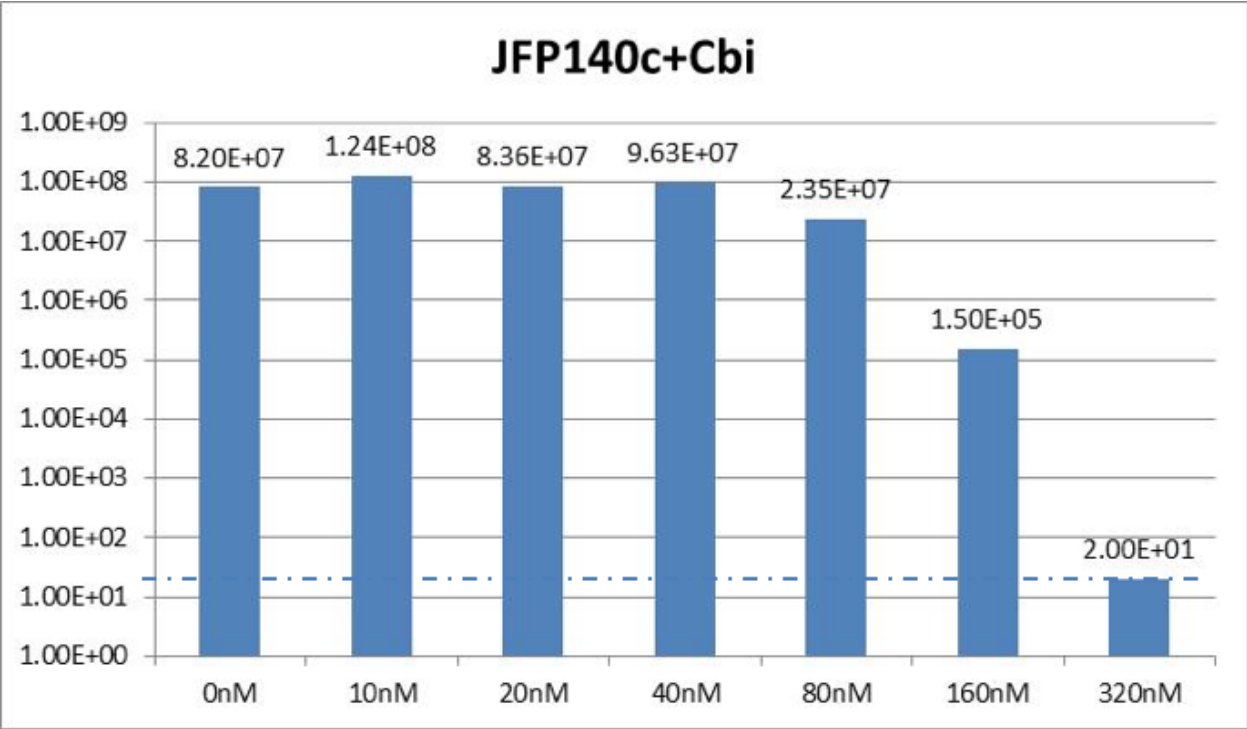


Figure 3. Effect of addition of Cbi on the growth of JFP140c (SM $\Delta nrdHEKF$, $nrdJ^+$). The x-axis is the Cbi concentration and the y-axis is the cfu/ml on a log scale. The 320 nM Cbi concentration was at the limit of detection (indicated by the dashed line).

Table 2 OD₆₆₀ Readings of JFP140c (SM Δ *nrdHEKF*, *nrdJ*⁺) with the addition of Cbi

Cbi conc. (nM)	OD₆₆₀			
	Expt. 1	Expt. 2	Expt. 3	Expt. 4
0	0.082	0.426	0.086	0.167
10	0.096	0.498		
15				0.180
20	0.103	0.315	0.121	0.199
25				0.157
30			0.112	
40	0.119	0.266		
80	0.065			
160	0.004			
320	0.000			

*Expt. 1 & 3 – 21 hours, Expt. 2 – 24 hours, Expt. 4 – 22 hours

JFP140c (*SM ΔnrdHEKF, nrdJ⁺*) failed to show an increase in growth when Cbi was added and Cbi actually had an inhibitory effect at higher concentrations. The failure to replicate the previous stimulation of growth could be due to Cbi being left out in room temperature when the experiment was performed previously. Being left at room temperature, the Cbi may have broken down into components that helped growth of JFP140c (*SM ΔnrdHEKF, nrdJ⁺*).

B. The Addition of Dimethylbenzimidazole (DMB)

It has been reported that *Salmonella enterica* can produce B₁₂ from Cbi only if DMB is also provided (32). Because of the slight increase in growth at 20 nM and 40 nM, 20 nM was used as the standard Cbi concentration while testing DMB concentrations. DMB was dissolved in 95% - 100% Ethanol (EtOH). To make sure that the EtOH was not affecting growth, a vehicle of 5 μL 95% - 100% EtOH was added to a control culture with no Cbi or DMB added. Five μL was chosen because no addition of DMB would exceed 5 μL. Concentrations were as follows: 0 nM Cbi, 0 nM DMB (control); 0 nM Cbi, 5 μL 95% - 100% EtOH (vehicle control); 20 nM Cbi, 0 nM DMB; 20 nM Cbi, 0.32 μM DMB; 20 nM Cbi, 150 μM DMB; 20 nM Cbi, 300 μM DMB (Table 3). All cultures and concentrations had 1 mM of IPTG added. DMB persistently inhibited growth of JFP140c (*SM ΔnrdHEKF, nrdJ⁺*) with increasing concentration. EtOH had no effect on growth of the cultures and was not a factor.

Table 3 OD₆₆₀ Readings of JFP140c (SM Δ *nrdHEKF*, *nrdJ*⁺) with the addition of Cbi and DMB

Cbi conc. & DMB conc.		OD ₆₆₀		
(nM)	(μ M)	Expt. 1	Expt. 2	Expt. 3
0 nM Cbi + 0 μ M DMB		0.178		0.204
0 nM Cbi + 5 μ L 100% EtOH*		0.183		0.221
20 nM Cbi + 0 μ M DMB		0.181	0.286	0.189
20 nM Cbi + 0.32 μ M DMB		0.169		0.142
20 nM Cbi + 150 μ M DMB		0.114	0.259	0.131
20 nM Cbi + 300 μ M DMB		0.072	0.160	0.092

*Vehicle control

C. Addition of Ethanolamine

Another potential way to stimulate B₁₂ production in the *nrdJ*⁺ mutants was to add ethanolamine. B₁₂ is needed to breakdown ethanolamine, and *S. sanguinis* has an ethanolamine utilization gene (*eut*) in close proximity to the B₁₂ biosynthetic pathway (*cob*). The addition of ethanolamine to the wild-type strain appeared to cause an increase in growth. At concentrations of 5 mM, 10 mM, 15 mM, 20 mM, 25 mM and 30 mM there was a definite increase in growth and a slight trend upward with the addition of higher concentrations of ethanolamine (Fig 4). This would suggest that the 70kb HGT region is producing coenzyme B₁₂ and that *eut* is working to some extent. A similar upward trend was also seen with JFP157 ($\Delta nrdI$, *nrdJ*⁺) when ethanolamine was added to the growth media. However, with JFP140 ($\Delta nrdHEKF$, *nrdJ*⁺) there was no increase in growth with ethanolamine. It should be noted that JFP157's ($\Delta nrdI$, *nrdJ*⁺) growth rate was much higher than JFP140 ($\Delta nrdHEKF$, *nrdJ*⁺) in oxygenated environments. This would seem to be contradictory with the previous tube assay (Fig 2). It is currently unknown why JFP157 ($\Delta nrdI$, *nrdJ*⁺) has a better growth rate than JFP140 ($\Delta nrdHEKF$, *nrdJ*⁺) in oxygenated BHI. JFP140c (SM $\Delta nrdHEKF$, *nrdJ*⁺) has a varied pattern of growth. At low OD₆₀₀ there was no increase in growth upon addition of ethanolamine. However, at higher OD₆₀₀ readings above 0.5, there was an increase in growth at low levels of ethanolamine 5 mM to 15 mM. Beyond 15 mM there was an inhibitory effect on the growth of JFP140c (SM $\Delta nrdHEKF$, *nrdJ*⁺).

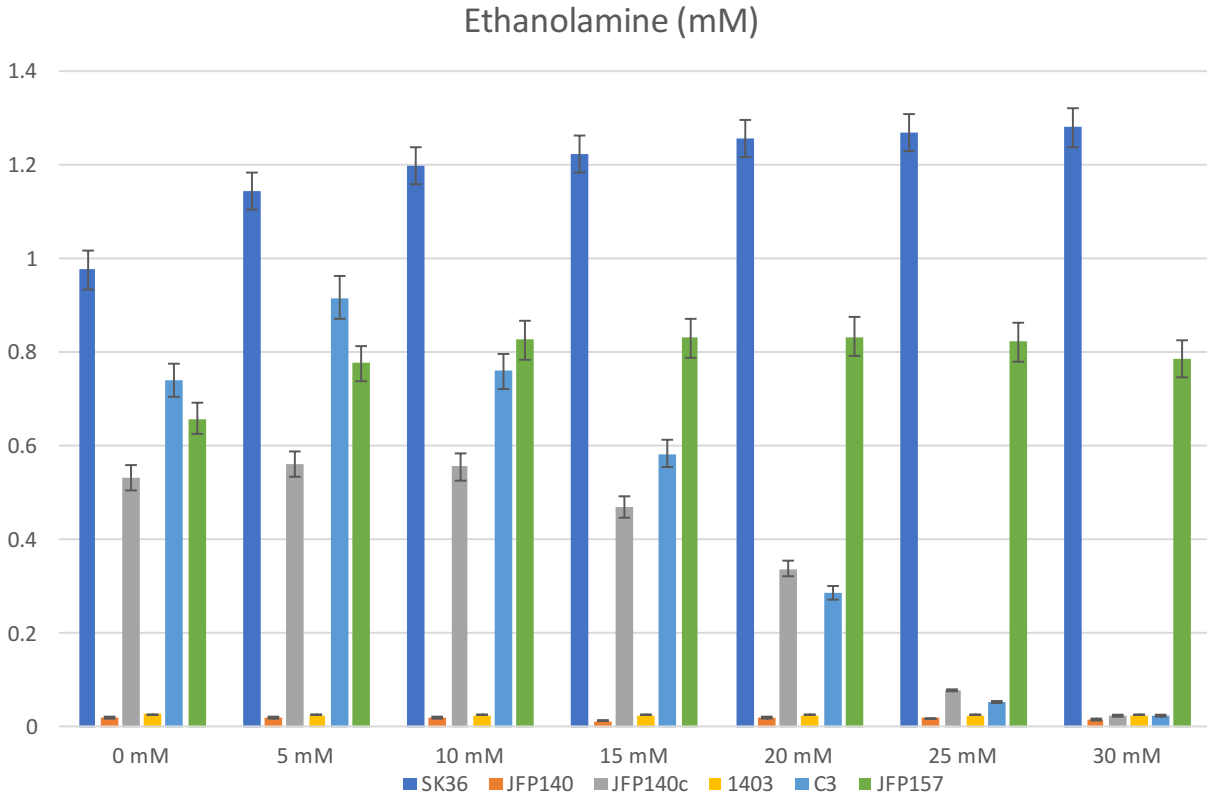


Figure 4. Addition of Ethanolamine to strains SK36 (WT), JFP140 ($\Delta nrdHEKF$, $nrdJ^+$), JFP140c (SM $\Delta nrdHEKF$, $nrdJ^+$), JFP157 ($\Delta nrdI$, $nrdJ^+$) and C3 (SM $\Delta nrdHEKF$, $\Delta nrdI$, $nrdJ^+$), and 1403 ($\Delta nrdHEKF$, $\Delta nrdI$, $nrdJ^+$). The x-axis is the ethanolamine concentration in mM and the y-axis is the OD₆₀₀ readings.

D. Gene SOEing to create $\Delta nrdHEKF$, $\Delta nrdI$, $nrdJ^+$

When JFP157 ($\Delta nrdI$, $nrdJ^+$) was tested with ethanolamine, it grew better than JFP140 ($\Delta nrdHEKF$, $nrdJ^+$), not just with the addition of ethanolamine but also without ethanolamine. The deletion of the gene *nrdI* from JFP140 ($\Delta nrdHEKF$, $nrdJ^+$) might have changed the growth pattern to be more like that of JFP157 ($\Delta nrdI$, $nrdJ^+$) or stayed similar to its parent JFP140 ($\Delta nrdHEKF$, $nrdJ^+$). The deletion of the gene *nrdI* from JFP140c (SM $\Delta nrdHEKF$, $nrdJ^+$), if the deletion did increase growth, could boost JFP140c (SM $\Delta nrdHEKF$, $nrdJ^+$) to WT levels. Using the gene SOEing technique, described in the materials and methods section, JFP140 ($\Delta nrdHEKF$, $nrdJ^+$) and JFP140c (SM $\Delta nrdHEKF$, $nrdJ^+$) had *nrdI* deleted and replaced with an erythromycin resistance cassette (*Erm^r*) (Fig 5). The double deletion mutant for JFP140 ($\Delta nrdHEKF$, $nrdJ^+$) was named 1403 ($\Delta nrdHEKF$, $\Delta nrdI$, $nrdJ^+$) and the double deletion mutant for JFP140c (SM $\Delta nrdHEKF$, $nrdJ^+$) was named C3 (SM $\Delta nrdHEKF$, $\Delta nrdI$, $nrdJ^+$) (Fig 6). This was done to see if the growth patterns would mimic JFP140 ($\Delta nrdHEKF$, $nrdJ^+$) or JFP157 ($\Delta nrdI$, $nrdJ^+$) using a tube assay to assess the growth pattern (Fig 6).

FORWARD PRIMERS

[A] (NrdIR3.2) AGCCATTGGTTGACCTTATCGTTAG->
 [B] (NrdIF2) CAACCGTAGGAACCTTGTGG->
 [C] (ErmF2.2) CCGGGCCCAAATTTGTTTGATTT->
 [D] (NrdIF3) TCTATTATTAACGGGAGGAAATAAGGTTTTCGTTTTTGATGT->
 [E] (NrdIF4) ATTGCGGCGGTTCAGTTTTG->

REVERSE PRIMERS

[F] (NrdIF1) GACGAAAGTCTGATGGAGTT->
 [G] (NrdIR2) GCTAAGAGCCAGATTGAAGCTAA->
 [H] (ErmR2.2) TTATTTCTCCCCTAAATAATAGATAACT->
 [I] (NrdIR1.2) CAAATCAAACAAATTTGGGCCCGGTCTAAAAAAT->
 [J] (NrdIR4) TGCATACTGGGATTTTGCTGG->

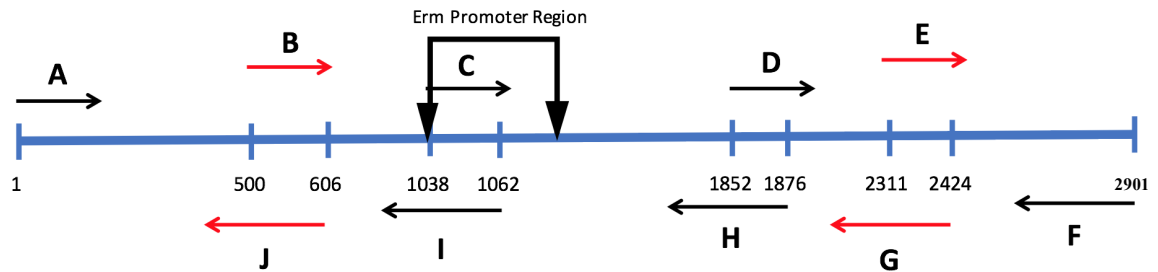


Figure 5. Gene SOEing diagram and primers for the creation of strains 1403 ($\Delta nrdHEKF$, $\Delta nrdI$, $nrdJ^+$) and C3 (SM $\Delta nrdHEKF$, $\Delta nrdI$, $nrdJ^+$). Primers A-J are indicated on the diagram with where the primers start. The Erm promoter region is indicated with the black closed arrows.

C3
SM
 $\Delta nrdHEKF,$
 $\Delta nrdI, nrdJ^+$

1403
 $\Delta nrdHEKF,$
 $\Delta nrdI, nrdJ^+$

SK36
WT

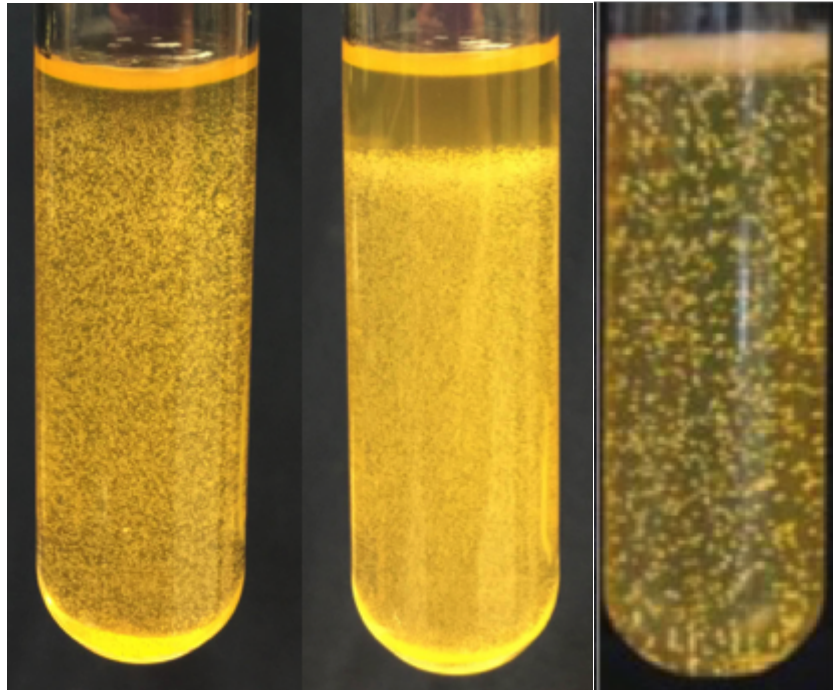


Figure 6. O₂ gradient tube assay using 1403 (*$\Delta nrdHEKF, \Delta nrdI, nrdJ^+$*) and C3 (SM *$\Delta nrdHEKF, \Delta nrdI, nrdJ^+$*). The tube assay for C3 (SM *$\Delta nrdHEKF, \Delta nrdI, nrdJ^+$*) and 1403 (*$\Delta nrdHEKF, \Delta nrdI, nrdJ^+$*) were done at the same time. SK36 (WT) was taken from Fig 2.

The strain 1403 ($\Delta nrdHEKF$, $\Delta nrdI$, $nrdJ^+$) grows similarly to JFP140 ($\Delta nrdHEKF$, $nrdJ^+$), in that it does not grow in the aerobic region. However, C3 (SM $\Delta nrdHEKF$, $\Delta nrdI$, $nrdJ^+$) grows much better than JFP140c (SM $\Delta nrdHEKF$, $nrdJ^+$) in the tube assay. C3 (SM $\Delta nrdHEKF$, $\Delta nrdI$, $nrdJ^+$) seems to grow almost to WT levels.

E. Ethanolamine effect on 1403 and C3

Strains 1403 ($\Delta nrdHEKF$, $\Delta nrdI$, $nrdJ^+$) and C3 (SM $\Delta nrdHEKF$, $\Delta nrdI$, $nrdJ^+$) were tested with ethanolamine to see how they compared to either JFP157 ($\Delta nrdI$, $nrdJ^+$) or JFP140 ($\Delta nrdHEKF$, $nrdJ^+$) and JFP140c (SM $\Delta nrdHEKF$, $nrdJ^+$). (Fig 4) The strain 1403 ($\Delta nrdHEKF$, $\Delta nrdI$, $nrdJ^+$) appeared similar to JFP140 ($\Delta nrdHEKF$, $nrdJ^+$) in both the standard growth study using BHI and also with the LMP tube assay. C3 (SM $\Delta nrdHEKF$, $\Delta nrdI$, $nrdJ^+$) grew to what seemed to be wild-type levels using the tube assay but the growth pattern in BHI broth was similar to JFP140c (SM $\Delta nrdHEKF$, $nrdJ^+$). When ethanolamine was added to the media the new mutants 1403 ($\Delta nrdHEKF$, $\Delta nrdI$, $nrdJ^+$) and C3 (SM $\Delta nrdHEKF$, $\Delta nrdI$, $nrdJ^+$) grew similarly to their parent strains. Growth of 1403 ($\Delta nrdHEKF$, $\Delta nrdI$, $nrdJ^+$) was not affected when ethanolamine was used and C3 (SM $\Delta nrdHEKF$, $\Delta nrdI$, $nrdJ^+$) showed a slight increase in growth at low levels 5 mM and 10 mM of ethanolamine and less growth at the higher levels, above 10 mM. Again, this rise and fall in growth was only at higher OD₆₀₀ readings while at lower readings, ethanolamine had no effect on the growth pattern.

F. Addition of 1,2-propanediol

Propanediol utilization genes (*pdu*) are also on the 70kb region with the B₁₂ biosynthetic pathway (*cob*) along with the ethanolamine utilization genes (*eut*). The addition of 1,2-propanediol could have resulted in a better growth increase than ethanolamine. However, 1,2-propanediol had no growth effect on the strains. There was no increase in growth even for the WT, SK36. JFP140 ($\Delta nrdHEKF$, $nrdJ^+$), JFP140c (SM $\Delta nrdHEKF$, $nrdJ^+$), 1403 ($\Delta nrdHEKF$, $\Delta nrdI$, $nrdJ^+$), C3 (SM $\Delta nrdHEKF$, $\Delta nrdI$, $nrdJ^+$) and JFP157 ($\Delta nrdI$, $nrdJ^+$) did not have an increase in growth and no inhibitory effects were observed with 1,2-propanediol (Fig 7).

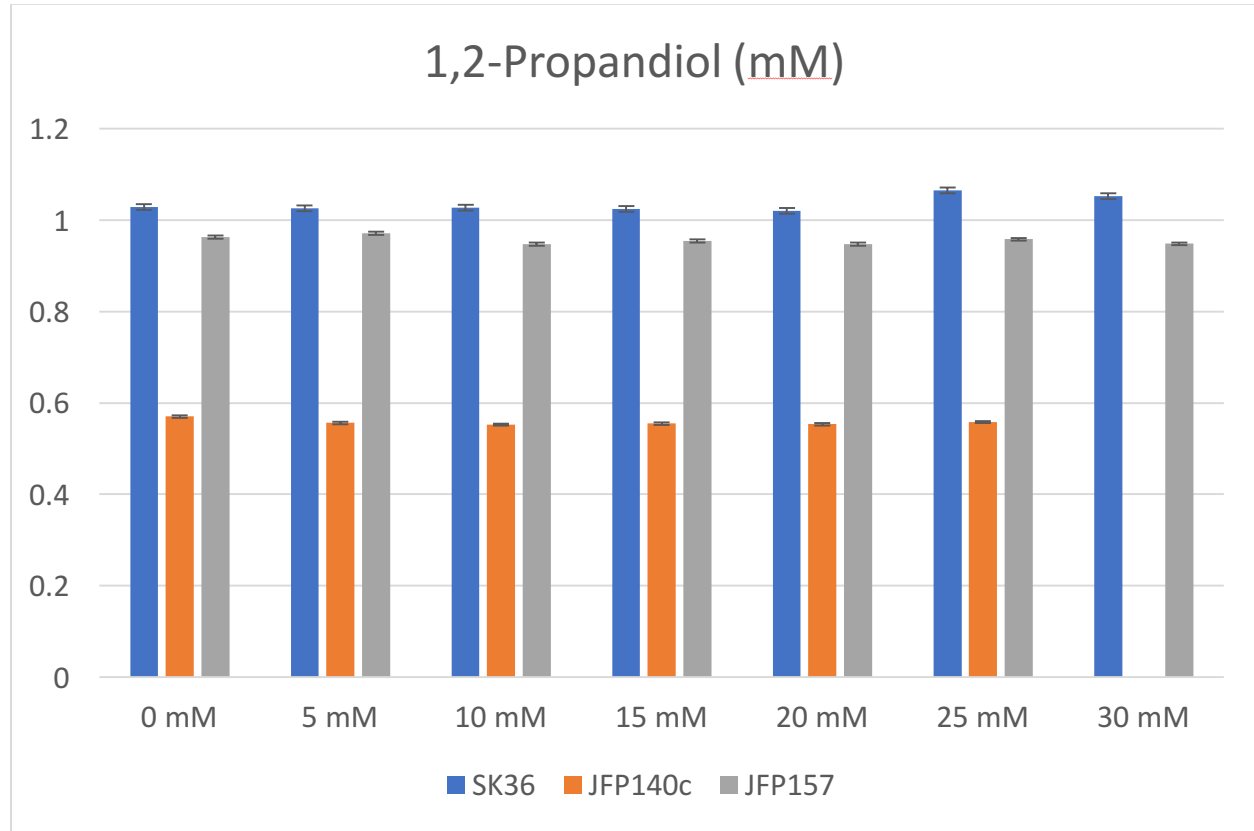


Figure 7. Addition of 1,2-propanediol to strains SK36 (WT), JFP140c (SM $\Delta nrdHEKF, nrdJ^+$), JFP157 ($\Delta nrdI, nrdJ^+$) and C3 (SM $\Delta nrdHEKF, \Delta nrdI, nrdJ^+$).

The x-axis is the 1,2-propandiol concentration in mM and the y-axis is the OD₆₀₀ readings.

G. Characterization of Spontaneous Mutants

The addition of Cbi, DMB, ethanolamine and 1,2-propanediol all failed to stimulate growth of the strains tested to WT levels. However, JFP140c (SM $\Delta nrdHEKF$, $nrdJ^+$) showed increased growth in the presence of oxygen compared to its parent JFP140 ($\Delta nrdHEKF$, $nrdJ^+$). This spontaneous suppressor mutant, containing a naturally occurring second mutation that reverts the phenotype of the first mutation, that may have been selected for by the addition of Cbi were hypothesized to have a secondary mutation that increases expression of the *nrdJ* gene or that increased production of coenzyme B₁₂. However, those ideas were just early speculations.

Another hypothesis of why JFP140c (SM $\Delta nrdHEKF$, $nrdJ^+$) grew better was because it was producing mini-cells without DNA. When extracting DNA from JFP140c (SM $\Delta nrdHEKF$, $nrdJ^+$) and JFP140 ($\Delta nrdHEKF$, $nrdJ^+$), more DNA was extracted from JFP140 ($\Delta nrdHEKF$, $nrdJ^+$) even though JFP140c (SM $\Delta nrdHEKF$, $nrdJ^+$) grew to higher OD levels. JFP140c (SM $\Delta nrdHEKF$, $nrdJ^+$) was hypothesized to be making mini-cells without DNA, which might have a higher OD₆₀₀. 4',6-diamidino-2-phenylindole (DAPI) staining was performed to see if this was true. The DAPI staining clearly indicates that JFP140c (SM $\Delta nrdHEKF$, $nrdJ^+$) does not have mini-cells. All JFP140c (SM $\Delta nrdHEKF$, $nrdJ^+$) cells have DNA within them (Fig 8).

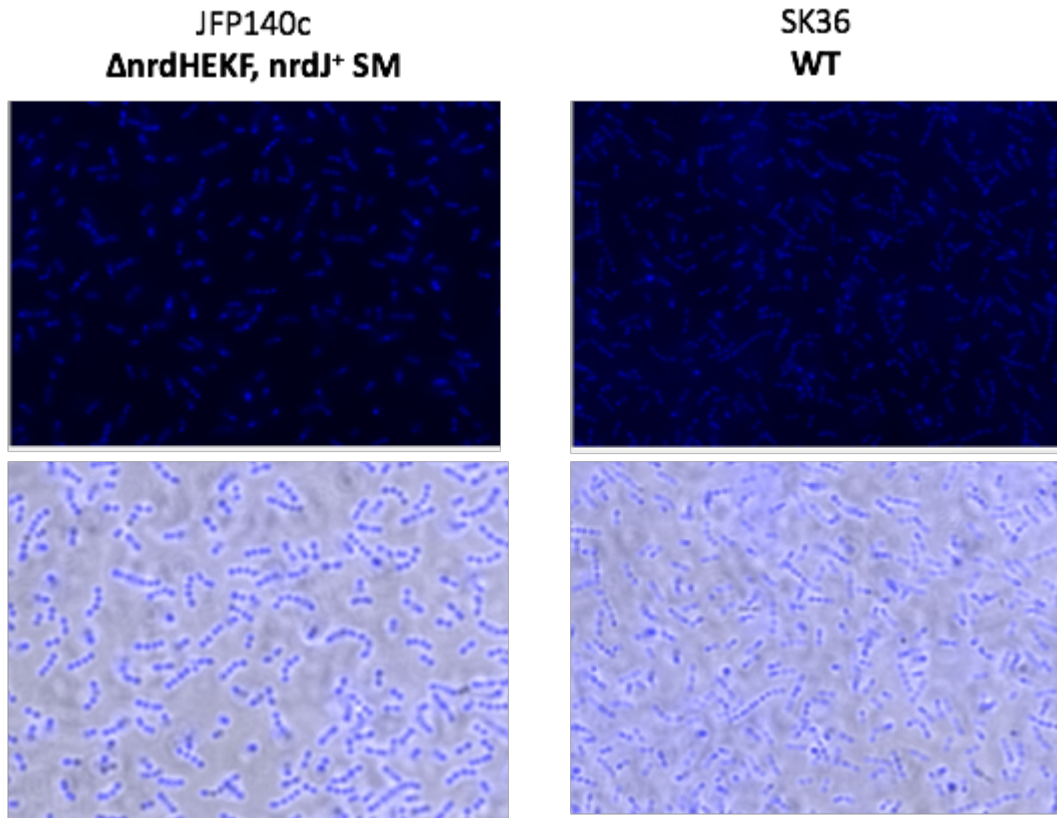


Figure 8. DAPI staining of JFP140c (SM $\Delta nrdHEKF, nrdJ^+$) and SK36 (WT). Pre-culture cells were grown anaerobically. Overnight cultures, which were inoculated with a 10^{-6} dilution of the pre-culture, were grown in 6% O_2 . DAPI (1:10,000) was added for 60 minutes and washed with PBS. Cells were viewed at 100x magnification with a Zeiss AxioObserver fluorescent microscope with an excitation wavelength of 365 nm and an emission of 445.

The creation of additional suppressor mutants (SM) that grow better than their parents, such as in the case of JFP140 ($\Delta nrdHEKF, nrdJ^+$) and JFP140c (SM $\Delta nrdHEKF, nrdJ^+$), could be beneficial. A collection of suppressor mutants with different mutations could be combined to create a strain that grows to WT levels without *nrdHEKF* and/or *nrdI* but with *nrdJ*. An LMP tube assay was used to identify other spontaneous suppressor mutants. As seen in Figure 2, some strains that were $\Delta nrdHEKF, nrdJ^+$ or $\Delta nrdI, nrdJ^+$ had growth in the aerobic portion of the tube. These colonies in the aerobic zone were hypothesized to be suppressor mutants.

Due to the favorable growth of JFP157 ($\Delta nrdI, nrdJ^+$), tube assays were made to collect colonies in the aerobic portion and to grow these colonies in LMP tubes and compare the parent from the potential suppressor mutant. Six potential suppressor mutants were created and stored for whole genome sequencing (Fig 9). All, the SM $\Delta nrdI, nrdJ^+$ were growing to near WT levels. There is however a “line” with limited growth at the boundary of the aerobic and anaerobic region.

To try to find other mutants, JFP163 ($\Delta nrdD, nrdJ^+$), which is deleted for the anaerobic RNR rather than the aerobic RNR, was tested to find suppressor mutants using tube assays also. Nine potential suppressor mutants were collected and stored for whole genome sequencing (Fig 10).

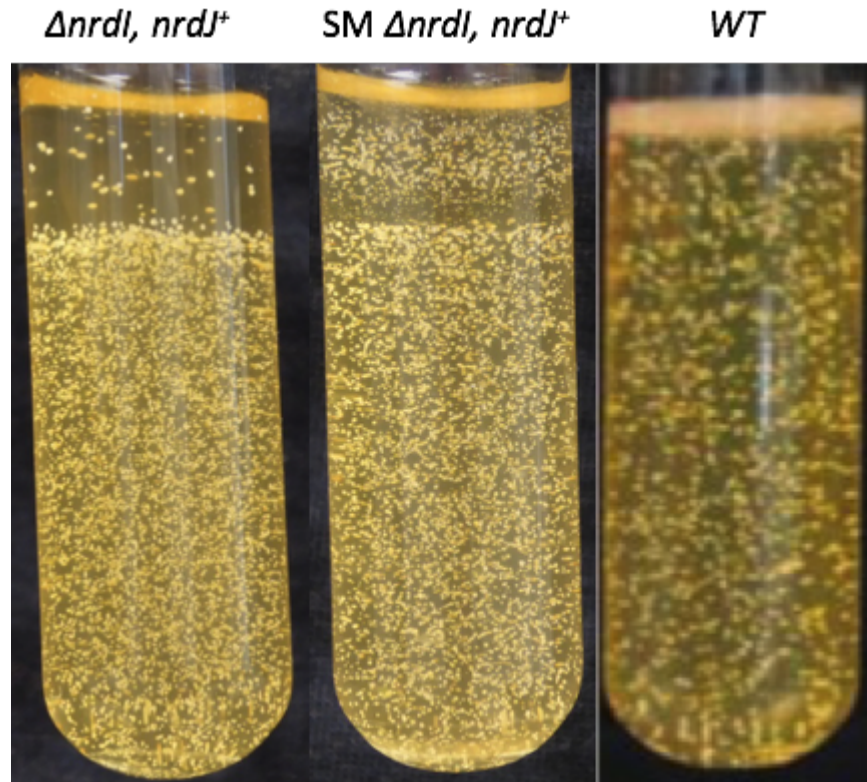


Figure 9. O₂ gradient tube assay using JFP157 ($\Delta nrdI, nrdJ^+$) and a potential SM of JFP157 (SM $\Delta nrdI, nrdJ^+$). SK36 (WT) was used as a reference and taken from Fig 2. The potential SM of JFP157 (SM $\Delta nrdI, nrdJ^+$) is in the middle. While JFP157 ($\Delta nrdI, nrdJ^+$) is on the left. All of the six SM JFP157 grew similarly to the middle photo.

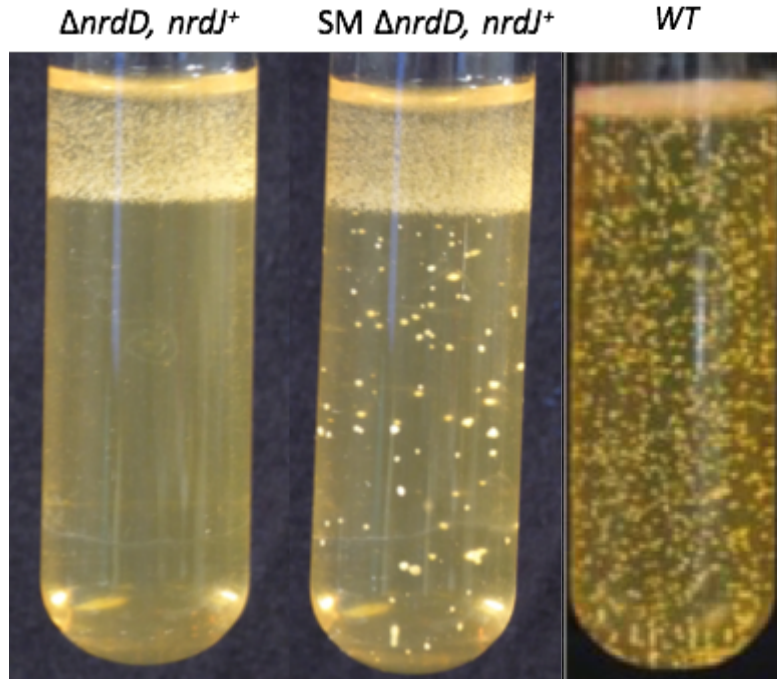


Figure 10. O₂ gradient tube assay using JFP163 ($\Delta nrdD, nrdJ^+$) and SM JFP163 1.1 (**SM $\Delta nrdD, nrdJ^+$**). SK36 (WT) was used as a reference and taken from Fig 2. The SM of JFP163 (SM $\Delta nrdD, nrdJ^+$) is in the middle. While JFP163 ($\Delta nrdD, nrdJ^+$) is on the left.

H. Whole-Genome Sequencing

After some potential spontaneous mutants, which grew better than their parent strains, were isolated, whole genome sequencing was performed to identify potential mutations within these strains. However, to make sure that the nucleotide changes observed, if any, were truly novel the parent strains were also sequenced including SK36 (WT) (Table 4). We wanted to understand why JFP140c (SM $\Delta nrdHEKF$, $nrdJ^+$) grows better than its parent JFP140 ($\Delta nrdHEKF$, $nrdJ^+$). Strains were sent off for sequencing. SK36 (WT) was re-sequenced to confirm its sequence and to potentially see any changes in the genome since sequencing it in 2007. JFP138 ($\Delta nrdHEKF$) was sequenced because it was the parent of JFP140 ($\Delta nrdHEKF$, $nrdJ^+$). JFP143 ($nrdI$) was sequenced because it was the parent of JFP157 ($\Delta nrdI$, $nrdJ^+$).

The sequencing and analysis were done by VCU Nucleic Acid Research Facilities - Genomics Core. Strains SK36 (WT), JFP140 ($\Delta nrdHEKF$, $nrdJ^+$), JFP140c (SM $\Delta nrdHEKF$, $nrdJ^+$), JFP138 ($\Delta nrdHEKF$) were sequenced by Illumina sequencing, Paired End Read, 2 x 300 bp MiSeq. To confirm our sequencing results, the prior strains were sequenced again and the new spontaneous suppressor mutants were also sequenced. They were also sequenced by Illumina sequencing, MiSeq, Paired End Read, 2 x 300 bp. However, analysis of the sequences was done with Geneious, a bioinformatic software program, within our lab.

There were no mutations found in any of the potential SM JFP157 (SM $\Delta nrdI$, $nrdJ^+$) when compared with the parent strain, JFP157 ($\Delta nrdI$, $nrdJ^+$). This failure to detect a mutation within SM JFP157 (SM $\Delta nrdI$, $nrdJ^+$) might be because the mutation,

if any, was in a region of the genome that contained repeats. One example would be in the tRNA and rRNA regions of the genome. In the potential suppressor mutants of JFP163 ($\Delta nrdD$, $nrdJ^+$), only one strain contained mutations. SM JFP163 1.1 (SM $\Delta nrdD$, $nrdJ^+$) had a single nucleotide polymorphism (SNP) in the *nox* gene, which was confirmed by Sanger sequencing (Fig 11). The *nox* gene encodes an NADH oxidase that can replenish NAD⁺ consumed during glycolysis at the expense of oxygen (35, 36). Also, JFP163 1.1 (SM $\Delta nrdD$, $nrdJ^+$) had an SNP in gene SSA_1239, which encodes a putative membrane protein (Fig 12). Finally, the only difference found in JFP140c (SM $\Delta nrdHEKF$, $nrdJ^+$) compared to JFP140 ($\Delta nrdHEKF$, $nrdJ^+$) was a single SNP in the fructose bisphosphate aldolase (*fba*) gene (Fig 13). This SNP was seen in two independent whole genome sequencing experiments.

Table 4 Strains that were whole genome sequenced with Illumina sequencing

Whole genome sequencing Strains	Description
SK36	Wild-Type (<i>Streptococcus sanguinis</i>)
JFP138	$\Delta nrdHEKF$
JFP143	$\Delta nrdI$
JFP140	$\Delta nrdHEKF, nrdJ^+$
JFP140c	SM $\Delta nrdHEKF, nrdJ^+$
C3	SM $\Delta nrdHEKF, \Delta nrdI, nrdJ^+$
JFP157	$\Delta nrdI, nrdJ^+$
JFP157 SM 1	Potential SM $\Delta nrdI, nrdJ^+$ #1
JFP157 SM 2	Potential SM $\Delta nrdI, nrdJ^+$ #2
JFP157 SM 3	Potential SM $\Delta nrdI, nrdJ^+$ #3
JFP157 SM 4	Potential SM $\Delta nrdI, nrdJ^+$ #4
JFP157 SM 5	Potential SM $\Delta nrdI, nrdJ^+$ #5
JFP157 SM 6	Potential SM $\Delta nrdI, nrdJ^+$ #6
JFP157 SM 7	Potential SM $\Delta nrdI, nrdJ^+$ #7
JFP163 clone 1	Clone 1 $\Delta nrdD, nrdJ^+$
JFP163 1.1	Clone 1 Potential SM $\Delta nrdD, nrdJ^+$ #1
JFP163 1.2	Clone 1 Potential SM $\Delta nrdD, nrdJ^+$ #2
JFP163 1.3	Clone 1 Potential SM $\Delta nrdD, nrdJ^+$ #3
JFP163 1.4	Clone 1 Potential SM $\Delta nrdD, nrdJ^+$ #4
JFP163 1.5	Clone 1 Potential SM $\Delta nrdD, nrdJ^+$ #5

JFP163 clone 2	Clone 2 $\Delta nrdD$, $nrdJ^+$
JFP163 2.1	Clone 2 Potential SM $\Delta nrdD$, $nrdJ^+$ #1
JFP163 2.2	Clone 2 Potential SM $\Delta nrdD$, $nrdJ^+$ #2
JFP163 2.3	Clone 2 Potential SM $\Delta nrdD$, $nrdJ^+$ #3
JFP163 2.4	Clone 2 Potential SM $\Delta nrdD$, $nrdJ^+$ #4

Nox in $\Delta nrdD$, $nrdJ^+$ *SM* (JFP163 Clone 1, SM 1)

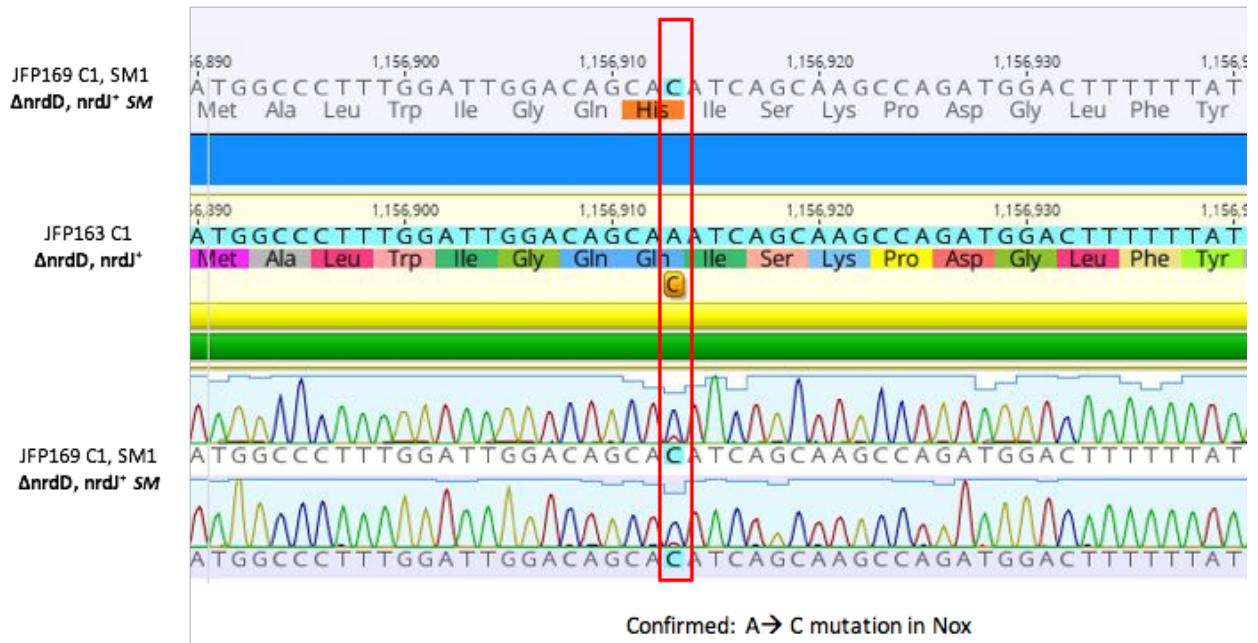
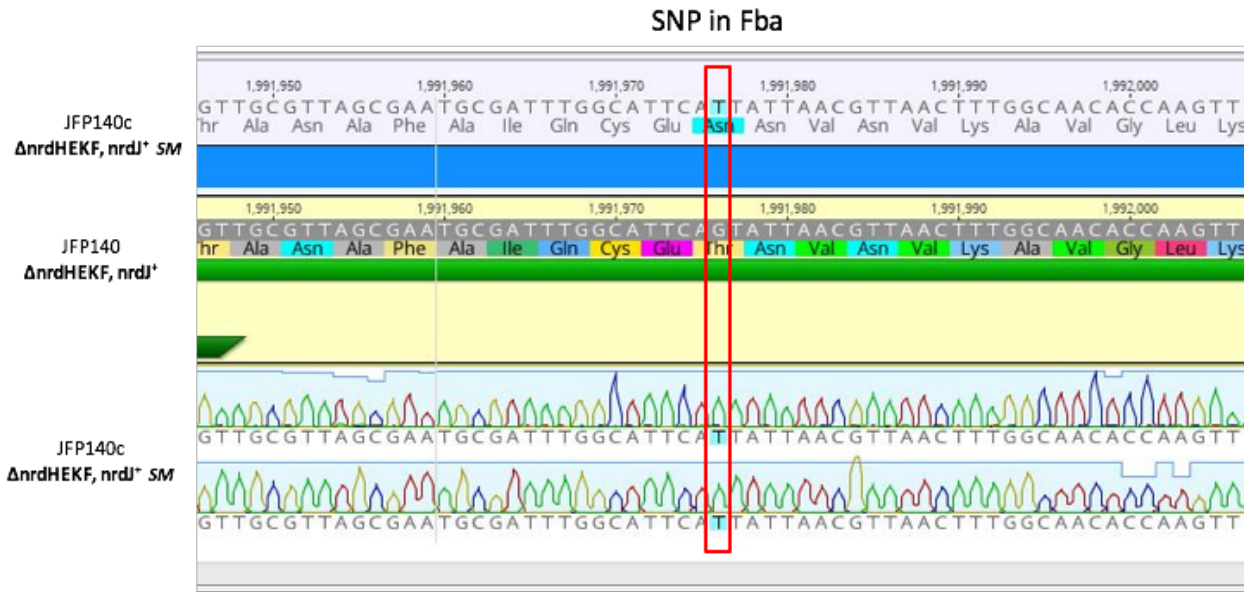


Figure 11. Genieious software image of the SNP in the *nox* gene for JFP169 1.1 (*SM* $\Delta nrdD$, $nrdJ^+$). The SNP within *nox* had an adenine replaced with a cytosine, highlighted with a red box. This changed the amino acid from a glutamine to a histidine.

SSA_1239 in $\Delta nrdD$, $nrdJ^+$ SM (JFP163 Clone 1, SM 1)



Figure 12. Genieous software image of the SNP in SSA_1239 for JFP169 1.1 (SM $\Delta nrdD$, $nrdJ^+$). The SNP within SSA_1239 had a cytosine replaced with a guanine, highlighted with a red box. This changed the amino acid from a tryptophan to a cysteine.



Confirmed: G → T mutation in Fba

Figure 13. Geneious software image of the SNP in Fba for JFP140c (SM $\Delta nrdHEKF, \Delta nrdI, nrdJ^+$). The SNP within Fba had a guanine replaced with a thymine, highlighted with a red box. This changed the amino acid from a threonine to an asparagine.

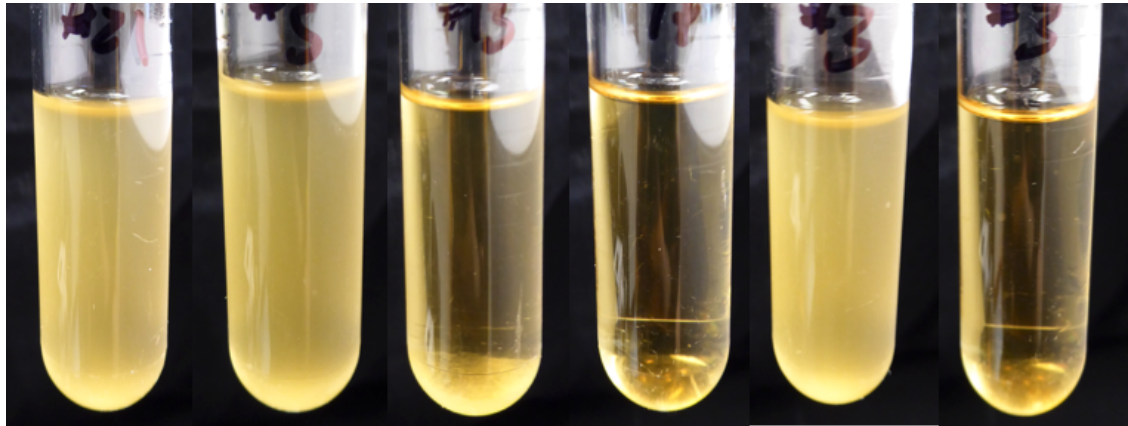
I. Transformation of JFP140 ($\Delta nrdHEKF$, $nrdJ^+$) with JFP140c (SM $\Delta nrdHEKF$, $nrdJ^+$) *fba* and JFP140c (SM $\Delta nrdHEKF$, $nrdJ^+$) with JFP140 ($\Delta nrdHEKF$, $nrdJ^+$) *fba*

The SNP in JFP140c's (SM $\Delta nrdHEKF$, $nrdJ^+$) *fba* gene was independently confirmed with whole genome sequencing to be the only mutational difference from JFP140 ($\Delta nrdHEKF$, $nrdJ^+$). To make sure this mutation truly caused the growth difference between JFP140 ($\Delta nrdHEKF$, $nrdJ^+$) and JFP140c (SM $\Delta nrdHEKF$, $nrdJ^+$), a transformation was performed to put JFP140's ($\Delta nrdHEKF$, $nrdJ^+$) *fba* into JFP140c (SM $\Delta nrdHEKF$, $nrdJ^+$) and JFP140c's *fba* into JFP140. Transformation was performed by the protocol described in the Materials and Methods section. Note that antibiotic selection was not used, so it was expected that the majority of colonies would not have taken up the DNA. Twenty-three colonies were picked for JFP140 ($\Delta nrdHEKF$, $nrdJ^+$) transformed with the *fba* variant from JFP140c (SM $\Delta nrdHEKF$, $nrdJ^+$) and grown in both 0% and 6% oxygenated BHI alongside controls of untransformed JFP140 ($\Delta nrdHEKF$, $nrdJ^+$) and JFP140c (SM $\Delta nrdHEKF$, $nrdJ^+$) in both 0% and 6% oxygen. Out of the twenty-three colonies picked, only seven grew to JFP140c (SM $\Delta nrdHEKF$, $nrdJ^+$) like levels. After sequencing the *fba* region with the SNP, only one sample contained the sequence of the JFP140c (SM $\Delta nrdHEKF$, $nrdJ^+$) *fba* gene.

Twenty-three samples were picked for JFP140c (SM $\Delta nrdHEKF$, $nrdJ^+$) transformed with the *fba* gene from JFP140 ($\Delta nrdHEKF$, $nrdJ^+$) and grown in both 0% and 6% oxygenated BHI with a control of JFP140 ($\Delta nrdHEKF$, $nrdJ^+$) and JFP140c (SM $\Delta nrdHEKF$, $nrdJ^+$) in both 0% and 6% oxygen also. Out of the twenty-three samples

only five seemed to grow like JFP140 ($\Delta nrdHEKF$, $nrdJ^+$). After sequencing the *fba* region with the SNP, only one sample contained the JFP140 ($\Delta nrdHEKF$, $nrdJ^+$) allele.

When the two transformed samples were grown with JFP140 ($\Delta nrdHEKF$, $nrdJ^+$) and JFP140c (SM $\Delta nrdHEKF$, $nrdJ^+$) for controls and with two failed transformants from JFP140c (SM $\Delta nrdHEKF$, $nrdJ^+$) transformed with JFP140 ($\Delta nrdHEKF$, $nrdJ^+$) *fba* and two from JFP140 ($\Delta nrdHEKF$, $nrdJ^+$) transformed with JFP140c (SM $\Delta nrdHEKF$, $nrdJ^+$) *fba*, the successful transformants had the same phenotype and growth pattern as the strain that was the source of the *fba* region (Fig 14). The mutation in the *fba* gene is therefore causal to the improved-growth phenotype of the JFP140c (SM $\Delta nrdHEKF$, $nrdJ^+$) suppressor mutant.



	[A]	[B]	[C]	[D]	[E]	[F]
Strain:	JFP140c	JFP140c	JFP140	JFP140	JFP140	JFP140c
Fba:	JFP140c	JFP140c	JFP140	JFP140	JFP140c	JFP140

Figure 14. Transformation of JFP140 ($\Delta nrdHEKF$, $nrdJ^+$) with JFP140c *fba* and JFP140c (SM $\Delta nrdHEKF$, $nrdJ^+$) with JFP140 *fba*. [A] is a failed transformation of JFP140c with JFP140 *fba*, numbered #21 (out of 23). [B] is a failed transformation of JFP140c with JFP140 *fba*, numbered #5 (out of 23). [C] is a failed transformation of JFP140 with JFP140c *fba*, numbered #13 (out of 23). [D] is a failed transformation of JFP140 with JFP140c *fba*, numbered #17 (out of 23). [E] is a successful transformation of JFP140 with JFP140c *fba*, numbered #3 (out of 23). [F] is a successful transformation of JFP140c with JFP140 *fba*, numbered #3 (out of 23).

J. Protein Structure of the Fba region in JFP140 ($\Delta nrdHEKF, nrdJ^+$) and JFP140c (SM $\Delta nrdHEKF, nrdJ^+$)

The mutation within JFP140c's (SM $\Delta nrdHEKF, nrdJ^+$) *fba* gene caused an amino acid change. To understand how the amino acid change affects the overall protein SWISS-MODEL (<https://swissmodel.expasy.org/>) was used to visualize the protein and its alignment to *Staphylococcus aureus*'s FBA (Fig 15 & Fig 16). The SNP changes a threonine into an asparagine. Both amino acids are polar with uncharged side chains but clearly this change causes the growth difference seen in JFP140 ($\Delta nrdHEKF, nrdJ^+$) and JFP140c (SM $\Delta nrdHEKF, nrdJ^+$). The SNP in JFP140c (SM $\Delta nrdHEKF, nrdJ^+$) was in an active site of FBA when compared to the *S. aureus* model (33).

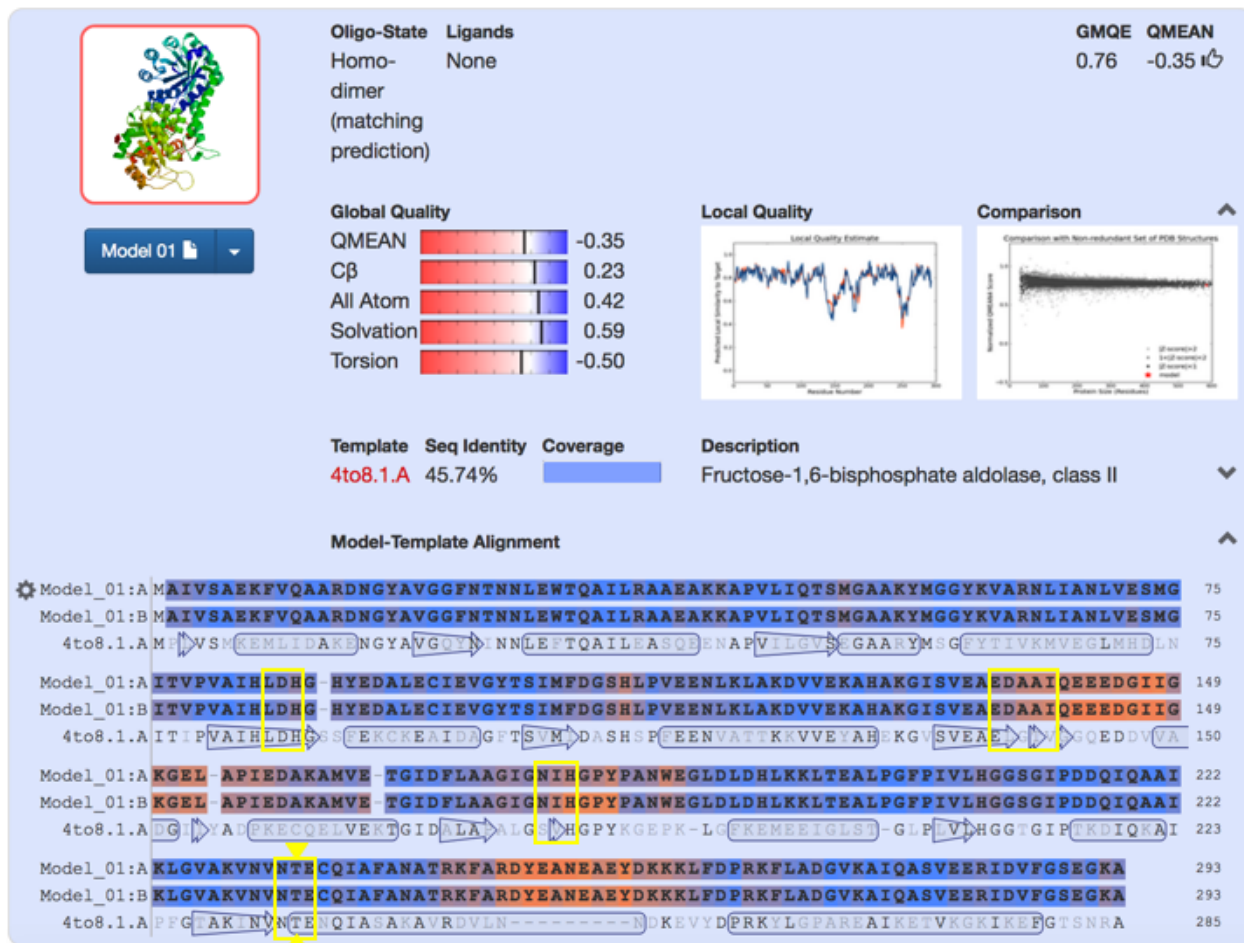


Figure 15. SWISS-MODEL used to make an alignment with JFP140 ($\Delta nrdHEKF$, $nrdJ^+$) and Methicillin-Resistant *Staphylococcus aureus* (4to8.1.A). The yellow boxes indicate the active sites of *S. aureus*'s Fba and the alignment to the Fba in JFP140 ($\Delta nrdHEKF$, $nrdJ^+$). The yellow triangles indicate the amino acid that was changed in JFP140c (SM $\Delta nrdHEKF$, $nrdJ^+$). Image was taken from SWISS-MODEL (<https://swissmodel.expasy.org/interactive/ue5PYL/models/>)

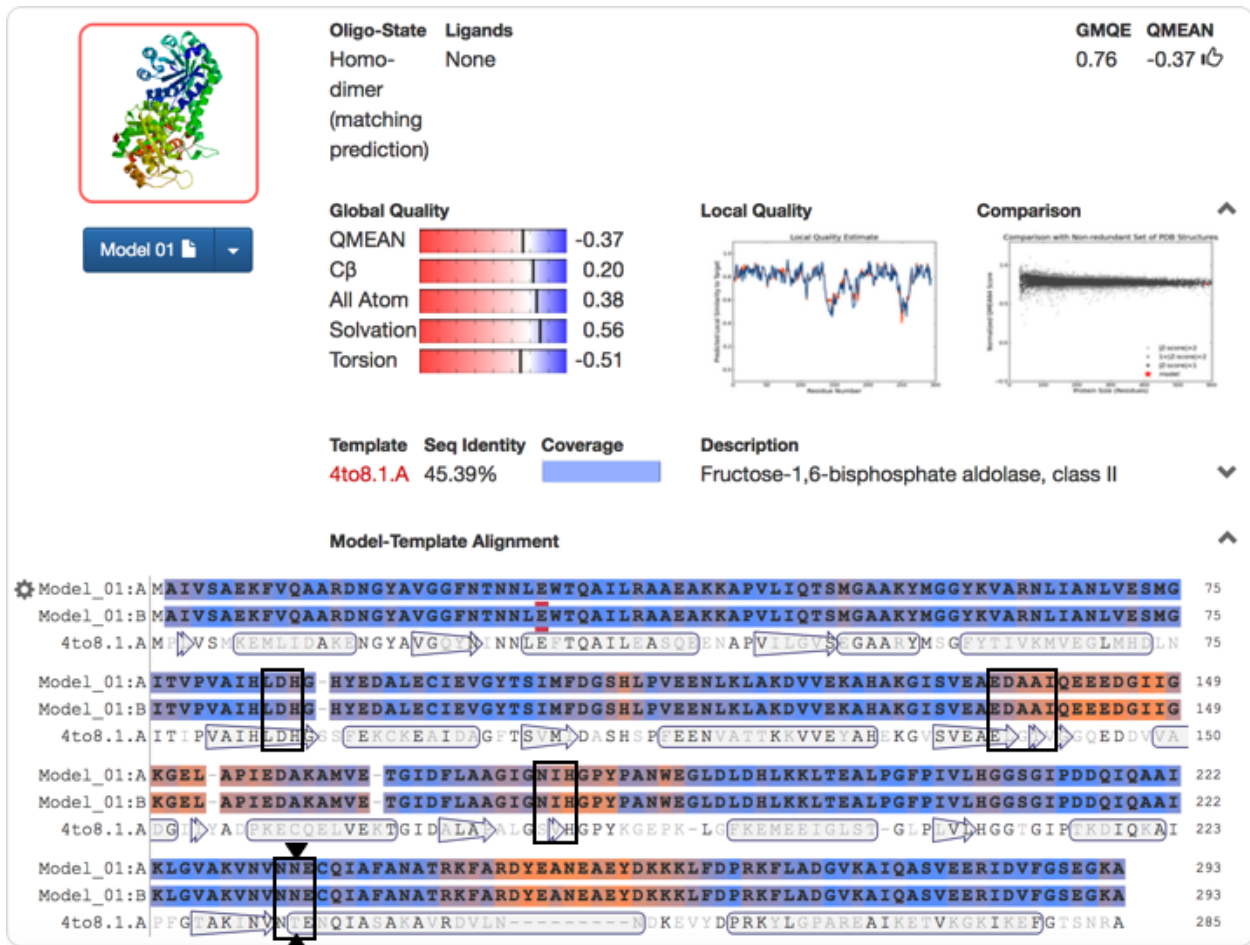


Figure 16. SWISS-MODEL used to make an alignment with JFP140c (SM $\Delta nrdHEKF$, $nrdJ^+$) and Methicillin-Resistant *Staphylococcus aureus* (4to8.1.A).

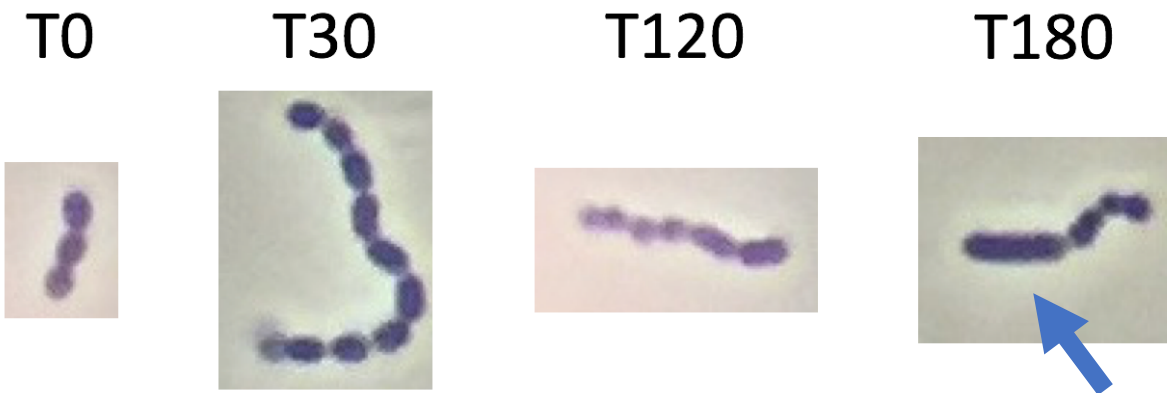
The black boxes indicate the active sites of *S. aureus*'s Fba and the alignment to the Fba in JFP140c (SM $\Delta nrdHEKF$, $nrdJ^+$). The black triangles indicate the amino acid that was changed in JFP140c (SM $\Delta nrdHEKF$, $nrdJ^+$). Image was taken from SWISS-MODEL (<https://swissmodel.expasy.org/interactive/rqmU8B/models/>)

K. Phenotypic comparison of SK36 (WT), JFP227 (Δ *ssaACB*, Δ SSA_1413) and JFP138 (Δ *nrdHEKF*)

If reduced activity of the manganese-dependent aerobic RNR is the reason why the Δ *ssaACB* mutant has reduced virulence, there might be phenotypic changes that are shared by both a manganese uptake mutant and the *nrdHEKF* mutant, JFP138 (Δ *nrdHEKF*). JFP227 (Δ *ssaACB*, Δ SSA_1413) was used rather than JFP169 (Δ *ssaACB*) because JFP227 (Δ *ssaACB*, Δ SSA_1413) has another apparent Mn transporter deleted, SSA_1413, in addition to Δ *ssaACB*, and is therefore more severely depleted for manganese. It was necessary to use this strain because although *ssaB* and *ssaACB* mutants grow poorly in low-Mn media when inoculated at low cell densities, their growth improves markedly when inoculated at the higher cell densities that are required for the biochemical analyses we had planned. (See below.)

SK36 (WT), JFP227 (Δ *ssaACB*, Δ SSA_1413) and JFP138 (Δ *nrdHEKF*) were all grown in BHI and stressed with oxygen using shaking baffled flasks. Under a light microscope at 100x, pictures were taken of the cells at time 0 minutes, 30 minutes, 120 minutes and 180 minutes. There is a phenotypic change with the introduction of oxygen causing an elongation of the cells of JFP227 (Δ *ssaACB*, Δ SSA_1413) and JFP138 (Δ *nrdHEKF*) (Fig 17).

JFP138 ($\Delta nrdHEKF$)



JFP227 ($\Delta ssaACB$, ΔSSA_{1413})



SK36 (WT)

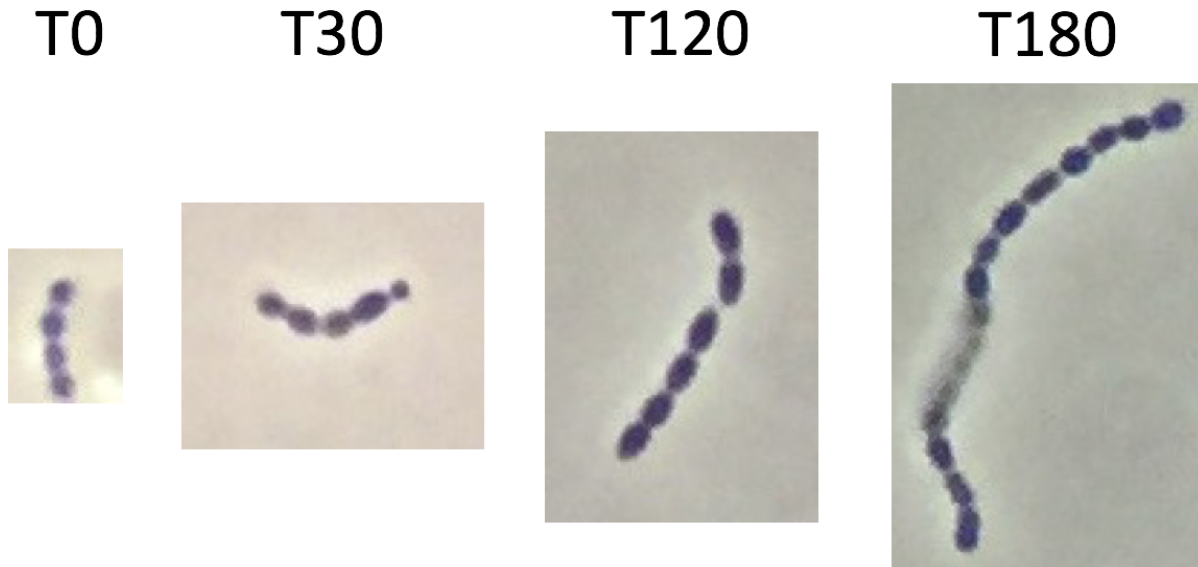


Figure 17. Phenotypic changes caused by oxygen stress over time on SK36 (WT), JFP227 (Δ *ssaACB*, Δ *SSA_1413*) and JFP138 (Δ *nrdHEKF*). Strains were transferred out of the anaerobic chamber into an aerobic shaker at 37°C. Time points are 0 minutes, viewed right after the cultures left the anaerobic chamber, 30 minutes, 120 minutes and 180 minutes, after strains were put in the shaker. Phase-contrast microscope was used at 100x.

L. Deoxynucleotide analysis of SK36 (WT), JFP138 ($\Delta nrdHEKF$) and JFP227 ($\Delta ssaACB, \Delta SSA_{1413}$)

Another test to see if the decrease in virulence from the lack of Mn was because of a deficiency in RNR, was to analyze the dNTP content of the strains. Strains were lysed prior to oxygen stress and two hours after oxygen stress to check dNTP levels. Analysis was done by Dr. Kim Baek's lab at Emory University.

Data are currently being generated.

IV. Discussion

This study had two goals. The first goal had two different approaches. The first goal was to create a mutant or create an environment in which the deleted class Ib RNR could be complemented with the class II RNR from *L. leichmannii*. The class II RNR was used because class Ia failed to work in the $\Delta nrdHEKF$ mutant (27). One way to do this would be to stimulate the native B₁₂ biosynthetic pathway to produce more B₁₂ for the *nrdJ*-containing mutants or by the addition of components of B₁₂, Cbi and DMB, to help alleviate the energy burden of creating B₁₂. The second way was to create a suppressor mutant that can grow to WT levels without the native aerobic RNR and with the class II RNR, NrdJ. The second goal was to compare the phenotypic characteristics and deoxyribonucleotide amounts of a Mn transporter mutant and the class Ib mutant ($\Delta nrdHEKF$).

S. sanguinis fails to grow aerobically with the deletion of the aerobic class Ib RNR. Ectopically expressing *nrdJ* in place of the missing RNR fails to completely complement activity of the native RNR. *S. sanguinis* has a 70kb-HGT region with a B₁₂ biosynthetic pathway and should produce coenzyme B₁₂, on the assumption that the bacteria would not have maintained such a large HGT region with no explanation. One thought of why *nrdJ* is not fully complementing is that the B₁₂ pathway is not producing enough B₁₂ or that the pathway is not being stimulated enough to work with the class II RNR. The addition of B₁₂ to the media might have helped with the stimulation of NrdJ activity; however, it is unknown if *S. sanguinis* has a B₁₂ transporter since none have

been found to date. The addition of B₁₂ components into the media, such as Cbi or DMB, failed to produce a positive growth response.

Addition of ethanolamine and 1,2-propanediol was used to stimulate B₁₂ production in *S. sanguinis* since the genes to utilize these two compounds are found on the same 70kb-HGT region. The addition of 1,2-propanediol failed to create a response in the strains tested, even WT. However, ethanolamine seemed to increase the growth of strains SK36 (WT), JFP40c (SM $\Delta nrdHEKF$, $nrdJ^+$) and JFP157 ($\Delta nrdI$, $nrdJ^+$) at higher OD₆₀₀ (> 0.5) readings. At the lower concentrations of ethanolamine, the growth seemed to be stimulated, but at higher levels the growth was inhibited. It is possible that at lower levels of ethanolamine, the B₁₂ biosynthetic pathway is stimulated to produce more B₁₂. The extra B₁₂ then is used by NrdJ to create more dNTPs and increases the growth of the strain. However, at higher concentrations, B₁₂ is consumed in the degradation of ethanolamine and B₁₂ is shunted away from NrdJ creating an inhibitory effect. Also, the biosynthetic pathways could have a limit to the amount of B₁₂ produced and only at low concentrations is the B₁₂ pathway stimulated with only a minimal amount of it going to the breakdown of ethanolamine. However, because SK36 (WT) showed an increase in growth and since SK36 (WT) has no need for B₁₂ to drive NrdJ activity, the increase in growth for all the strains must be due to the breakdown products of ethanolamine. Ethanolamine must be providing a carbon or nitrogen source that is increasing growth. B₁₂ is most likely not being shunted to NrdJ.

Potentially, the growth deficiency of the *nrdJ*-containing strain could nevertheless be from the lack of sufficient B₁₂. The insertion of a B₁₂ transporter from *Bacillus subtilis*

or *Enterococcus faecalis* could reveal if the lack of B₁₂ is definitively the cause of the *nrdJ* mutants' failure to grow to WT levels. This could be a future experiment.

Cbi had an inhibitory effect at high concentrations while DMB had no effect on growth; even when used in combination, both failed to produce an increase in growth. The strain JFP140c (SM $\Delta nrdHEKF$, *nrdJ*⁺), which was thought to be able to use Cbi to increase growth, was found to be a suppressor mutant with a single SNP in the Fba protein that changes an amino acid in the active site, as seen in *S. aureus* (33).

Sequencing has revealed that a single SNP is the only apparent difference between JFP140 ($\Delta nrdHEKF$, *nrdJ*⁺) and JFP140c (SM $\Delta nrdHEKF$, *nrdJ*⁺). By transforming the region with the mutation, the WT into the mutant and vice versa, it affirmed that the change of the nucleotide was the reason for the growth differences. Also, because C3 (SM $\Delta nrdHEKF$, $\Delta nrdI$, *nrdJ*⁺) grows similarly to JFP140c (SM $\Delta nrdHEKF$, *nrdJ*⁺) in broth cultures yet better in the tube assay, C3 (SM $\Delta nrdHEKF$, $\Delta nrdI$, *nrdJ*⁺) could be a better choice to evolve into a strain that grows to WT levels without a Mn-dependent RNR. Fba is a protein that uses Zn and its increase in growth should not be connected to Mn. Fba is an enzyme catalyzing a reversible reaction that splits, fructose 1,6-bisphosphate, into the triose phosphates dihydroxyacetone phosphate (DHAP) and glyceraldehyde 3-phosphate (G3P). The fact that the growth of JFP140c (SM $\Delta nrdHEKF$, *nrdJ*⁺) was improved by mutation of the *fba* gene rather than of a gene or regulator of the B₁₂ biosynthetic region may indicate that the failure of the *nrdJ*-containing strain to grow as well as a *nrdHEKF*-containing strain is not due to inadequate levels of cellular B₁₂. Further studies will be required to determine why the

mutation of the *fba* gene improves aerobic growth of the *nrdJ*-complemented *nrdHEKF* mutant (JFP140c).

We know Fba is the reason that JFP140c (SM $\Delta nrdHEKF$, *nrdJ*⁺) has a better growth rate than JFP140 ($\Delta nrdHEKF$, *nrdJ*⁺) and we can form a new hypothesis on why JFP140c (SM $\Delta nrdHEKF$, *nrdJ*⁺) had a high OD reading but a low DNA yield. The products of Fba feed into cell wall synthesis (38). Alteration of Fba's activity might therefore conceivably thicken the peptidoglycan layer, making the cells harder to lyse, which would explain the lower DNA yield obtained from the Fba suppressor mutant. It is not yet clear why this change would improve the aerobic growth of the suppressor mutant. Alternatively, Fba has been classified as a "moonlighting protein", meaning that it has functions unrelated to glycolysis (37). Thus, it's possible that the mutation improves growth and/or reduces DNA yield by modifying an unknown function of Fba.

The phenotypic changes seen in JFP138 ($\Delta nrdHEKF$) and JFP227 ($\Delta ssaACB$, ΔSSA_1413) were similar. Both strains had exaggerated elongation of cells at longer time points after oxygen stress (>2 hours). This could be morphological evidence that the shortage of Mn that prevents growth of uptake mutants in Mn-limited environments also reduces the activity of the aerobic Mn dependent RNR. This failure allows for the cells to elongate but fail to divide from the lack of dNTPs to replicate and/or repair DNA.

The analysis of the dNTPs from the lysates of SK36 (WT), JFP138 ($\Delta nrdHEKF$) and JFP227 ($\Delta ssaACB$, ΔSSA_1413) should reveal a better understanding of whether lack of dNTPs because of deletion of *nrdHEKF* is the reason why the decrease in Mn causes *S. sanguinis* to lose its virulence.

Deletion of *ssaACB*, a Mn transporter, decreased virulence of *S. sanguinis*. Mn is somehow important to aerobic virulence. SodA, within *S. sanguinis*, is a superoxide dismutase that uses Mn. SodA seemed like an obvious reason why the cell would need Mn in oxygen; however, the deletion of SodA did reduce virulence but not to the same extent as the deletion of *ssaACB* (25). This means that Mn is used for something within *S. sanguinis* that is more critical than superoxide dismutase.

A crucial system that uses Mn in *S. sanguinis* is the native class Ib RNR. The deletion of RNR causes a massive loss in virulence in *S. sanguinis*. In the animal studies, the $\Delta nrdHEKF$ mutant could not be recovered from the animal after 20 hours. Even the DNA was unrecoverable (27). This makes this mutant the most incapacitated mutant seen so far. This suggests that the aerobic class Ib RNR might be a good drug target.

Even though NrdHEKF is a good drug target and *S. sanguinis* is highly incapacitated, it is still unknown if the decrease in Mn from the *ssaACB* is due to decreased RNR activity from the lack of Mn. It is entirely possible that Mn is needed for another system or enzyme, besides RNR, that is the true reason why the decrease in Mn causes a decrease in virulence. More work must be done to definitively say whether RNR is or is not the true reason why the deletion of the Mn transporter, *ssaACB*, causes a loss in virulence.

1. Billroth, T. (1874). *Untersuchungen über die Vegetationsformen von Coccobacteria septica und der Antheil, welchen sie an der Entstehung und Verbreitung der accidentellen Wundkrankheiten haben*. Berlin: G. Reimer.
2. Billroth, T. (1877). *Lectures on surgical pathology and therapeutics*. London: The New Sydenham Society.
3. Alouf J. E., Horaud T. Streptococcal Research at Pasteur Institute from Louis Pasteur's time to date. *Advances in Experimental Medicine and Biology*. 1997;418:7–14. PubMed PMID: 9331588.
4. Ferretti J, Köhler W. History of Streptococcal Research. 2016 Feb 10. In: Ferretti JJ, Stevens DL, Fischetti VA, editors. *Streptococcus pyogenes* : Basic Biology to Clinical Manifestations [Internet]. Oklahoma City (OK): University of Oklahoma Health Sciences Center; 2016-.
5. Schottmuller H. Die Artunterscheidung der für den Menschen pathogenen Streptokokken durch Blutagar. *Münchener med Wochenschrift*. 1903;50:848–853909-912.
6. Becker W. C. The necessity of a standard blood-agar plate for the determination of hemolysis by streptococci. *Journal of Infectious Diseases*. 1916;19(6):754–759.
7. Lancefield, R. C. (1933). A serological differentiation of human and other groups of hemolytic streptococci. *The Journal of Experimental Medicine*, 57(4), 571–595.
8. Sherman, J. M. (1937). The streptococci. *Bacteriological Reviews*, 1(1), 3–97.

9. Truper, H. and L. D. Clari. 1997. Taxonomic note: necessary corrections of specific epithets formed as substantives (nouns) “in apposition”. *Int. J. Syst. Bacteriol.* 47:908-909.
10. Caufield, P. W., Dasanayake, A. P., Li, Y., Pan, Y., Hsu, J., & Hardin, J. M. (2000). Natural History of *Streptococcus sanguinis* in the Oral Cavity of Infants: Evidence for a Discrete Window of Infectivity. *Infection and Immunity*, 68(7), 4018–4023.
11. Nyvad, B., and M. Kilian. 1987. Microbiology of the early colonization of human enamel and root surfaces in vivo. *Scand. J. Dent. Res.* 95:369-380.
12. Kolenbrander PE, London J. Adhere today, here tomorrow: oral bacterial adherence. *J Bacteriol.* 1993; 175:3247–3252. [PubMed: 8501028]
13. Kreth, J., Merritt, J., Shi, W., & Qi, F. (2005). Competition and Coexistence between *Streptococcus mutans* and *Streptococcus sanguinis* in the Dental Biofilm. *Journal of Bacteriology*, 187(21), 7193–7203.
<http://doi.org/10.1128/JB.187.21.7193-7203.2005>
14. P. Moreillon and Y.-A. Que, Infective endocarditis, *The Lancet*, vol. 363, no. 9403, pp. 139–149, 2004.
15. Senty Turner, L., Das, S., Kanamoto, T., Munro, C. L., & Kitten, T. (2009). Development of genetic tools for in vivo virulence analysis of *Streptococcus sanguinis*. *Microbiology*, 155(Pt 8), 2573–2582.
<http://doi.org/10.1099/mic.0.024513-0>
16. Paik, S., Senty, L., Das, S., Noe, J. C., Munro, C. L., & Kitten, T. (2005). Identification of Virulence Determinants for Endocarditis in *Streptococcus*

- sanguinis* by Signature-Tagged Mutagenesis. *Infection and Immunity*, 73(9), 6064–6074. <http://doi.org/10.1128/IAI.73.9.6064-6074.2005>
17. Wallace, S. M., Walton, B. I., Kharbanda, R. K., Hardy, R., Wilson, A. P., & Swanton, R. H. (2002). Mortality from infective endocarditis: clinical predictors of outcome. *Heart*, 88(1), 53–60.
18. Douglas C.W.I., Heath J., Hampton K.K., Preston F.E., Identity of viridans streptococci isolated from cases of infective endocarditis, *J. Med. Microbiol.* 39 (1993) 179–182.
19. Infective endocarditis: an epidemiological review of 128 episodes. C. Dyson, R. A. Barnes, G. A. Harrison *J Infect.* 1999 March; 38(2): 87–93.
20. Das, S., Kanamoto, T., Ge, X., Xu, P., Unoki, T., Munro, C. L., & Kitten, T. (2009). Contribution of Lipoproteins and Lipoprotein Processing to Endocarditis Virulence in *Streptococcus sanguinis*. *Journal of Bacteriology*, 191(13), 4166–4179. <http://doi.org/10.1128/JB.01739-08>
21. Facklam, R. (2002). What Happened to the Streptococci: Overview of Taxonomic and Nomenclature Changes. *Clinical Microbiology Reviews*, 15(4), 613–630. <http://doi.org/10.1128/CMR.15.4.613-630.2002>
22. Sherman, J. M. (1937). The Streptococci. *Bacteriological Reviews*, 1(1), 3–97.
23. Clarridge, J. E. (2004). Impact of 16S rRNA Gene Sequence Analysis for Identification of Bacteria on Clinical Microbiology and Infectious Diseases. *Clinical Microbiology Reviews*, 17(4), 840–862. <http://doi.org/10.1128/CMR.17.4.840-862.2004>

24. Kitten, T., Munro, C. L., Michalek, S. M., & Macrina, F. L. (2000). Genetic Characterization of a *Streptococcus mutans* Lral Family Operon and Role in Virulence. *Infection and Immunity*, 68(8), 4441–4451.
25. Crump, K. E., Bainbridge, B., Brusko, S., Turner, L. S., Ge, X., Stone, V., ... Kitten, T. (2014). The Relationship of the Lipoprotein SsaB, Manganese, and Superoxide Dismutase in *Streptococcus sanguinis* Virulence for Endocarditis. *Molecular Microbiology*, 92(6), 1243–1259. <http://doi.org/10.1111/mmi.12625>
26. Torrents, E. (2014). Ribonucleotide reductases: essential enzymes for bacterial life. *Frontiers in Cellular and Infection Microbiology*, 4, 52. <http://doi.org/10.3389/fcimb.2014.00052>
27. Rhodes, D. V., Crump, K. E., Makhlynets, O., Snyder, M., Ge, X., Xu, P., Stubbe, J., Kitten, T. (2014). Genetic Characterization and Role in Virulence of the Ribonucleotide Reductases of *Streptococcus sanguinis*. *The Journal of Biological Chemistry*, 289(9), 6273–6287. <http://doi.org/10.1074/jbc.M113.533620>
28. Shisler, K. A., & Broderick, J. B. (2014). Glycyl radical activating enzymes: Structure, mechanism, and substrate interactions. *Archives of Biochemistry and Biophysics*, 546, 64–71. <http://doi.org/10.1016/j.abb.2014.01.020>
29. Makhlynets, O., Boal, A. K., Rhodes, D. V., Kitten, T., Rosenzweig, A. C., & Stubbe, J. (2014). *Streptococcus sanguinis* Class Ib Ribonucleotide Reductase: high activity with both iron and manganese cofactors and structural insights. *The Journal of Biological Chemistry*, 289(9), 6259–6272. <http://doi.org/10.1074/jbc.M113.533554>

30. Xu, P., Alves, J. M., Kitten, T., Brown, A., Chen, Z., Ozaki, L. S., ... Buck, G. A. (2007). Genome of the Opportunistic Pathogen *Streptococcus sanguinis*. *Journal of Bacteriology*, 189(8), 3166–3175. <http://doi.org/10.1128/JB.01808-06>
31. J.R. Mellin, M. Koutero, D. Dar, M.A. Nahori, R. Sorek, P. Cossart
Riboswitches. Sequestration of a two-component response regulator by a
riboswitch-regulated noncoding RNA. *Science*, 345 (2014), pp. 940–943
32. Anderson, P. J., Lango, J., Carkeet, C., Britten, A., Kräutler, B., Hammock, B. D.,
& Roth, J. R. (2008). One Pathway Can Incorporate either Adenine or
Dimethylbenzimidazole as an α -Axial Ligand of B₁₂ Cofactors in *Salmonella*
enterica. *Journal of Bacteriology*, 190(4), 1160–1171.
<http://doi.org/10.1128/JB.01386-07>
33. Capodagli, G. C., Lee, S. A., Boehm, K. J., Brady, K. M., & Pegan, S. D. (2014).
Structural and Functional Characterization of Methicillin-Resistant
Staphylococcus aureus's Class IIb Fructose 1,6-Bisphosphate Aldolase.
Biochemistry, 53(48), 7604–7614. <http://doi.org/10.1021/bi501141t>
34. Horton R. PCR-mediated recombination and mutagenesis. SOEing together
tailor-made genes. *Mol. Biotechnol*, 1995;3(2):93-9. doi: 10.1007/BF02789105
35. Ge, X., Yu, Y., Zhang, M., Chen, L., Chen, W., Elrami, F., Kong, F., Kitten, T.,
and Xu, P. (2016). Involvement of NADH oxidase in competition and endocarditis
virulence in *Streptococcus sanguinis*. *Infect Immun*. 84: 1470-1477.
36. Ge, X., Shi, X., Shi, L., Liu, J., Stone, V., Kong, F., Kitten, T., and Xu, P. (2016).
Involvement of NADH oxidase in biofilm formation in *Streptococcus sanguinis*.
PLoS ONE. 11: e0151142.

37. Shams F., Oldfield N. J., Wooldridge K. G. & Turner D. P. J. Fructose-1,6-bisphosphate aldolase (FBA)—a conserved glycolytic enzyme with virulence functions in bacteria: 'Ill met by moonlight'. *Biochem. Soc. Trans.* 42, 1792–1795 (2014).
38. Xu, P., Ge, X., Chen, L., Wang, X., Dou, Y., Xu, J. Z., ... Buck, G. A. (2011). Genome-wide essential gene identification in *Streptococcus sanguinis*. *Scientific Reports*, 1, 125. <http://doi.org/10.1038/srep00125>

VITA

John Lee Smith was born on October 19, 1987 in Newport News, VA. He graduated from West Springfield High School in Springfield, VA in 2006. He received his Bachelor of Art in Religious Studies from the University of Mary Washington in 2012. He also received his Bachelor of Science in Biology from Virginia Commonwealth University in 2015. He has been accepted into Virginia Commonwealth University Dental School Class of 2021.